Molecular Phylogenetics and Evolution 201 (2024) 108199

Contents lists available at ScienceDirect

Molecular Phylogenetics and Evolution

journal homepage: www.elsevier.com/locate/ympev

Deciphering the evolution and biogeography of ant-ferns *Lecanopteris* s.s

Li-Ju Jiang [a,1], Jing Zhao [b,1], Jia-Guan Wang [b,1], Sven Landrein [c], Ji-Pu Shi [a], Chuan-Jie Huang [b], Miao Luo [b], Xin-Mao Zhou [b,*], Hong-Bin Niu [a,*], Zhao-Rong He [d,*]

[a] Gardening and Horticulture Centre, Xishuangbanna Tropic Botanical Garden, Chinese Academy of Sciences, Mengla 666303, Yunnan, China
[b] School of Ecology and Environmental Science, Yunnan University, Kunming 650504, Yunnan, China
[c] Kadoorie Farm and Botanic Garden, Lam Kam Road, Tai Po, New Territories, Hong Kong Special Administrative Region of China
[d] School of Life Sciences, Yunnan University, East Outer Ring Road, Chenggong District, Kunming 650500, Yunnan, China

ARTICLE INFO

Keywords:
Ant plants
Nothotaxa
Microsoroideae
Islands
Dispersal
Incomplete lineage sorting

ABSTRACT

Southeast Asia is a biodiversity hotspot characterized by a complex paleogeography, and its Polypodiopsida flora is particularly diverse. While hybridization is recognized as common in ferns, further research is needed to investigate the relationship between hybridization events and fern diversity. *Lecanopteris* s.s., an ant-associated fern, has been subject to debate regarding species delimitations primarily due to limited DNA markers and species sampling. Our study integrates 22 newly generated plastomes, 22 transcriptomes, and flow cytometry of all native species along with two cultivated hybrids. Our objective is to elucidate the reticulate evolutionary history within *Lecanopteris* s.s. through the integration of phylobiogeographic reconstruction, gene flow inference, and genome size estimation. Key findings of our study include: (1) An enlarged plastome size (178–187 Kb) in *Lecanopteris* s.s., attributed to extreme expansion of the Inverted Repeat (IR) regions; (2) The traditional 'pumila' and 'crustacea' groups are paraphyletic; (3) Significant cytonuclear discordance attributed to gene flow; (4) Natural hybridization and introgression in the 'pumila' and 'darnaedii' groups; (5) *L. luzonensis* is the maternal parent of *L.* 'Yellow Tip', with *L. pumila* suggested as a possible paternal parent; (6) *L.* 'Tatsuta' is a hybrid between *L. luzonensis* and *L. crustacea*; (7) *Lecanopteris* s.s. first diverged during the Neogene and then during the middle Miocene climatic optimum in the Indochina and Sundaic regions. In conclusion, the biogeographic history and speciation of *Lecanopteris* have been profoundly shaped by past climate changes and geodynamics of Southeast Asia. Dispersals, hybridization and introgression between species act as pivotal factors in the evolutionary trajectory of *Lecanopteris* s.s.. This research provides a robust framework for further exploration and understanding of the complex dynamics driving the diversification and distribution patterns within Polypodiaceae subfamily Microsoroideae.

1. Introduction

Southeast Asia is a biodiversity hotspot which may be a consequence of its complex past geodynamics (Myers et al., 2000; Buerki et al., 2014). Buerki et al. (2014) have proposed that the Southeast Asia region is one of the origins and refuges of early-diverging lineages of plants by integrated palaeobotanical evidence, phylogenetic relationships, molecular dating inferences, and biogeography results. However, few studies have focused on specific families or genera of ferns in Southeast Asia. Reconstructing the phylobiogeography of fern taxa that occupy this region could give a better understanding of how land plants diversified in this area, and molecular dating allows us to determine whether evolutionary events coincide with historical tectonic or climatic events in a particular region (Pillon, 2012; Fay and Forest, 2013; Richardson et al., 2014).

Hybridization has been recognized as an important mechanism in evolution of plants and is particularly common in ferns (Wood et al., 2009; Liu et al., 2020). However, further studies on how hybridization contributed to fern speciation and phylogeography are needed. Most known documented natural hybrids are from temperate lineages and it was suggested that hybridization was rare or at least less common in tropical epiphytic ferns (Yatabe et al., 2001; Kreier and Schneider, 2006; Liu et al., 2020). Liu et al. (2020) provided a comprehensive evaluation of ferns and lycophytes nothotaxa in the context of PPG I (2016). In their

* Corresponding authors.
E-mail addresses: xinmao.zhou@ynu.edu.cn (X.-M. Zhou), niuhongbin@xtbg.ac.cn (H.-B. Niu), zhrhe@ynu.edu.cn (Z.-R. He).
[1] Co-first authors.

https://doi.org/10.1016/j.ympev.2024.108199
Received 28 April 2024; Received in revised form 3 September 2024; Accepted 11 September 2024
Available online 14 September 2024

work, five temperate lineages of ferns showed a much higher diversity of nothospecies than another five lineages which mostly or exclusively occurred in tropical zones (Liu et al., 2020). The observed difference may be the results from the biased concentration of botanical institutions and research in the northern hemisphere (Liu et al., 2020). This suggests a need to expand research in the tropical regions such as Indochina, Malesia, Philippines, and so on.

Ants have been living alongside plants for at least 140 million years (Moreau et al., 2006; Nelsen et al., 2018). They engage with various parts of plants, forming relationships such as defensive mutualisms and seed dispersal (Campbell et al., 2023). These interactions have been found in five fern families with extrafloral nectaries or domatia (Koptur, 1992). Several genera of Polypodiaceae, such as *Platycerium* Desv. (Platycerioideae) and *Microgramma* C. Presl (Polypodioideae) (Hennipman and Roos, 1983; Almeida, 2018), have developed a relationship with ants similar to that seen in some epiphytic Angiosperms of the families Rubiaceae and Apocynaceae. The ferns provide a living space for the ants in swollen rhizomes, nest fronds, or tubers, and some of the ferns may also provide food for the ants (Koptur, 1992). The ants, in return, could provide nutrients for the plants (Davidson and McKey, 1993). *Lecanopteris* s.s. Reinw. (Polypodiaceae subfam. Microsoroideae), is an ant-associated fern genus and comprises ca. 13 epiphytic species in tropical Southeast Asia and mostly confined to Malesia. Only one species [*L. sinuosa* (Wall. ex Hook.) Copel.) is widespread and can be found in Thailand, Cambodia, Vietnam, Australia, Vanuatu, and the Solomon Islands (Gay et al., 1994). This genus is characterized by a hollow or expanded rhizome that is used as a nest site by ants (Gay, 1993a, b). *Lecanopteris* s.s. has been shown to benefit nutritionally from the faeces and debris left by the ants (Gay, 1993a, b). Several in-depth studies have explored the ant mutualism in *Lecanopteris* s.s., however, the species relationships and delimitations are still not well resolved (Haufler et al., 2003; Testo et al., 2019).

There are contrasting results regarding the taxonomy of lecanopteroid ferns (*Lecanopteris* s.s. and its sister genera) (PPG I, 2016; Testo et al., 2019; Chen et al., 2020; Perrie et al., 2021; Wei and Zhang, 2022). At the genus level, Chen et al. (2020) proposed three possible genus ranks classification: (1) four genera (*Bosmania* Testo [three species], *Dendroconche* Copel. [eight species], *Zealandia* Testo & A.R. Field [four species], and *Lecanopteris* s.s. [13 species]); (2) three genera (*Bosmania*, *Zealandia*, and *Lecanopteris* [including *Dendroconche*]); (3) two genera (*Bosmania* Testo and *Lecanopteris* s.l. [including *Dendroconche*, *Zealandia*]). Perrie et al. (2021) discussed the advantages and disadvantages of these different approaches, and provide the new combinations in *Lecanopteris* s.l. required for the third option. In addition, Perrie et al. (2021) recognized *Lecanopteris* s.l. including 24 species, one with two subspecies, occurring mainly found in Malesia and Australasia, but extending to Thailand, Cambodia, Vietnam, and some western Pacific Islands as eastward as Fiji. However, Testo et al. (2019) and Wei & Zhang (2022) supported the four genera and 13 species classification of lecanopteroid ferns. Within the *Lecanopteris* s.s., Ching (1940) suggested that *Lecanopteris* s.s. could be divided into two genera: *Lecanopteris*, and *Myrmecophila* Christ ex Nakai (=*Myrmecopteris* Pic. Serm.). In this study, we decided to focus on *Lecanopteris* sensu stricto (13 species) which does not include *Dendroconche* (8 species) and *Zealandia* (4 species). Gay et al. (1994) and Hennipman & Hovenkamp (1998) recognised two subgenera within *Lecanopteris* s.s.: subg. *Lecanopteris* (divided into the informal 'pumila' group and the 'darnaedii' group including *L. darnaedii*, *L. holttumii*, and *L. spinosa*), and subg. *Myrmecopteris* (corresponding to the informal 'crustacea' group including *L. crustacea*, *L. sarcopus*, *L. lomarioides*, *L. sinuosa*, and *L. mirabilis*). Although diverse leaf and rhizome features have provided numerous autapomorphic characters for diagnosing species, there are few shared derived characters (Gay et al., 1994; Hennipman and Hovenkamp, 1998).

Previous phylogenetic studies have improved our understanding of the evolutionary history among *Lecanopteris* s.s. members to a certain extent, but a well-resolved phylogenetic framework of the genus *Lecanopteris* s.s. has not been explored to date due to the limited DNA markers and inadequate species sampling (Haufler et al., 2003 [11 samples; two plastid markers]; Kreier et al., 2008 [12 samples; four plastid markers]; Wei et al., 2017 [2 samples; three plastid markers]; Testo et al., 2019 [12 samples; four plastid markers]; Chen et al., 2020, 2021 [4–8 samples; four or six plastid markers]). Haufler et al. (2003) first reconstructed the phylogenetic relationships among 11 species of *Lecanopteris* s.s. based on the analysis of two plastid markers (*rbc*L, *trn*L-F). The results are highly incongruent with those circumscribed by Gay et al. (1994) based on the basis of morphological data. Besides, some species-level relationships were not resolved or were only weakly supported (bootstrap values = 55–100) (Haufler et al., 2003). Kreier et al. (2008) inferred the relationships of *Lecanopteris* s.s. with weak to strong support (ML-BS = 0–100; MP-JK = 0–100; BI-PP = 0–1.0) based on a concatenated four plastid markers (*rbc*L, *rps*4, *rps*4-*trn*S, and *trn*L-F). Recently, twelve species of *Lecanopteris* s.s. were included in a phylogenetic analysis focused on the genus *Lecanopteris* s.l. on the basis of four plastid markers (*rbc*L, *rps*4, *rps*4-*trn*S, and *trn*L-F) (Testo et al., 2019), the species-level relationships within *Lecanopteris* s.s. were also mostly not strongly supported (ML-BS = 59–100; BI-PP = 0.74–1.00).

In this study, *Lecanopteris* s.s. was used as an example group based on a comprehensive set of methodologies combining phylobiogeographic reconstruction (using transcriptome orthologs genes and the complete plastomes), phylogenomic conflicts, gene flow inference, and flow cytometry. Our aims were to (1) characterize the plastomes of *Lecanopteris* s.s. species; (2) infer species relationships based on different datasets; (3) trace the origin of two cultivated hybrids (*L.* 'Yellow Tip', and *L.* 'Tatsuta') by identifying their parents; (4) examine the causes of the phylogenomic incongruence; (5) how past distribution and climatic changes in Southeast Asia may have facilitated reticulate evolution.

2. Materials and methods

2.1. Data compilation and sampling

22 Samples representing all accepted native species and two cultivated hybrids of *Lecanopteris* s.s. were sampled for this study. Except for two cultivated hybrids (*L.* 'Yellow Tip', and *L.* 'Tatsuta'), remaining material were collected from the wild, all samples are grown and maintained in the Xishuangbanna Tropical Botanical Garden (XTBG). For each sample, voucher specimens were deposited in the herbarium of Xishuangbanna Tropical Botanical Garden of the Chinese Academy of Sciences (HITBC) and Yunnan University (PYU). Fresh and healthy leaf material was divided into three parts, one part was collected and dried in silica gel for genome skimming sequencing, and the other two parts were flash frozen in liquid nitrogen for transcriptome sequencing and flow cytometry. Plastome sequences of 57 species and transcriptome raw data of 13 accessions of 12 species were downloaded from NCBI as outgroups. Therefore, incorporating 22 newly generated plastomes, a total of 79 assembled plastome sequences representing ca. 75 fern species, 3 subfamilies, and 12 genera (Wei and Zhang, 2022) were included in the final plastome (PT) dataset (Table 1). For the transcriptome analysis, the final (TT) dataset included 35 accessions representing ca. 28 species, 3 subfamilies, and 9 genera were included (Table 2; Wei and Zhang, 2022)

2.2. DNA extraction, sequencing, plastome assembly, and annotation

Total genomic DNA was extracted from silica gel-dried leaves material using an improved Cetyl Trimethyl Ammonium Bromide (CTAB) method (Doyle, 1987). The extracted DNA was subsequently sheared into 300–500-bp fragments for library construction. Paired-end (PE) reads (2 × 150 bp) were sequenced on an Illumina Nova6000 platform at BioMaker Technology Co., Ltd. (Beijing, China). Fastp v0.23.1 (Chen et al., 2018) was used to trim adapters and remove low-quality reads, generating approximately 2 Gb of clean PE reads per sample. The plastomes were assembled from the clean reads using GetOrganelle v1.7.5.3

Table 1
List of plastomes used in this study.

Subfamily	Species	Voucher	GenBank ID	Cities
Drynarioideae	***Selliguea mairei*** (Brause) X.C. Zhang & L.J. He	X.C. Zhang 4609 (PE)	MW876364	Wei et al., 2021
Microsoroideae	***Bosmania membranacea*** (D. Don) Testo	Cheng X. et al. FB541 (KUN)	MT130574	Du et al., 2021
Microsoroideae	***Bosmania membranacea*** subsp. ***carinata*** (W.M. Chu & Z.R. He) R. Wei & X.C. Zhang	R. Wei WR0410 (PE)	MW876308	Wei et al., 2021
Microsoroideae	***Bosmania membranacea*** subsp. ***membranacea*** (D. Don) Testo	R. Wei WR0368 (PE)	MW876309	Wei et al., 2021
Microsoroideae	***Goniophlebium amoenum*** (Wall. ex Mett.) Bedd.	Z.Y. Li 1897 (PE)	MW876318	Wei et al., 2021
Microsoroideae	***Goniophlebium argutum*** (Wall. ex Hook.) J.Sm. ex Hook.	R. Wei ST465 (PE)	MW876319	Wei et al., 2021
Microsoroideae	***Goniophlebium chinensis*** (Christ) S. G. Lu	Cheng X. et al. FB186 (KUN)	MT130566	Du et al., 2021
Microsoroideae	***Goniophlebium formosanum*** (Baker) Rodl-Linder,	X.C. Zhang 9432 (PE)	MW876320	Wei et al., 2021
Microsoroideae	***Goniophlebium manmeiense*** (Christ) Rodl-Linder	X.P. Qi Q061 (PE)	MW876321	Wei et al., 2021
Microsoroideae	***Goniophlebium mengtzeense*** (Christ) Rodl-Linder	H.M. Liu GX211 (PE)	MW876322	Wei et al., 2021
Microsoroideae	***Goniophlebium niponicum*** (Mett.) Bedd.	H.M. Liu A305 (PE)	MW876323	Wei et al., 2021
Microsoroideae	***Goniophlebium persicifolium*** (Desv.) Bedd.	X.C. Zhang 433 (PE)	MW876324	Wei et al., 2021
Microsoroideae	***Lecanopteris balgooyi*** Hennipman	JZW-AF7 (PYU, HITBC)	PP496839	This study
Microsoroideae	***Lecanopteris carnosa*** (Reinw.) Blume	JZW-AF19 (PYU, HITBC)	PP496851	This study
Microsoroideae	***Lecanopteris celebica*** Hennipman	JZW-AF18 (PYU, HITBC)	PP496850	This study
Microsoroideae	***Lecanopteris crustacea*** Copel. −1	JZW-AF1 (PYU, HITBC)	PP496833	This study
Microsoroideae	***Lecanopteris crustacea*** Copel. −2	JZW-AF2 (PYU, HITBC)	PP496834	This study
Microsoroideae	***Lecanopteris darnaedii*** Hennipman	JZW-AF12 (PYU, HITBC)	PP496844	This study
Microsoroideae	***Lecanopteris deparioides*** (Ces.) Baker −1	JZW-AF4 (PYU, HITBC)	PP496836	This study
Microsoroideae	***Lecanopteris deparioides*** (Ces.) Baker −2	JZW-AF5 (PYU, HITBC)	PP496837	This study
Microsoroideae	***Lecanopteris holttumii*** Hennipman	JZW-AF10 (PYU, HITBC)	PP496842	This study
Microsoroideae	***Lecanopteris lomarioides*** (Kunze ex Mett.) Copel.	JZW-AF21 (PYU, HITBC)	PP496853	This study
Microsoroideae	***Lecanopteris luzonensis*** Hennipman −1	JZW-AF9 (PYU, HITBC)	PP496841	This study
Microsoroideae	***Lecanopteris luzonensis*** Hennipman −2	JZW-AF11 (PYU, HITBC)	PP496843	This study
Microsoroideae	***Lecanopteris luzonensis*** Hennipman −3	JZW-AF22 (PYU, HITBC)	PP496854	This study
Microsoroideae	***Lecanopteris mirabilis*** Copel. −1	JZW-AF3 (PYU, HITBC)	PP496835	This study
Microsoroideae	***Lecanopteris mirabilis*** Copel. −2	JZW-AF15 (PYU, HITBC)	PP496847	This study
Microsoroideae	***Lecanopteris pumila*** Blume ex Copel.	JZW-AF6 (PYU, HITBC)	PP496838	This study
Microsoroideae	***Lecanopteris sarcopus*** (Teijsm. & Binn.) Copel.	JZW-AF20 (PYU, HITBC)	PP496852	This study
Microsoroideae	***Lecanopteris sinuosa*** (Wall. ex Hook.) Copel. −1	JZW-AF14 (PYU, HITBC)	PP496846	This study
Microsoroideae	***Lecanopteris sinuosa*** (Wall. ex Hook.) Copel. −2	JZW-AF16 (PYU, HITBC)	PP496848	This study
Microsoroideae	***Lecanopteris spinosa*** Jermy & T. Walker	JZW-AF8 (PYU, HITBC)	PP496840	This study
Microsoroideae	***Lecanopteris*** 'Tatsuta'	JZW-AF17 (PYU, HITBC)	PP496849	This study
Microsoroideae	***Lecanopteris*** 'Yellow Tip'	JZW-AF13 (PYU, HITBC)	PP496845	This study
Microsoroideae	***Lepisorus affinis*** Ching	Wei Q. et al. FB787 (KUN)	MT130664	Du et al., 2021
Microsoroideae	***Lepisorus carnosus*** (J.Sm.) C.F. Zhao, R. Wei & X.C. Zhang	Wei Q. WQ439 (KUN)	MT130559	Du et al., 2021
Microsoroideae	***Lepisorus carnosus*** (J.Sm.) C.F. Zhao, R. Wei & X.C. Zhang	Cult. (FLBG)	MN623356	Liu et al., 2020
Microsoroideae	***Lepisorus clathratus*** (C.B. Clarke) Ching	jingB-1 (PE)	KY419704	Wei et al., 2017
Microsoroideae	***Lepisorus confluens*** W. M. Chu	Cheng X. et al. FB174 (KUN)	MT130651	Du et al., 2021
Microsoroideae	***Lepisorus fortuni*** (T. Moore) C. M. Kuo	SS Liu 201,630 (SYS)	NC056109	Liu et al., 2020
Microsoroideae	***Lepisorus hederaceus*** (Christ) R. Wei & X.C. Zhang	Cult. (WBG)	MN623364	Liu et al., 2020
Microsoroideae	***Lepisorus jakonensis*** (Blanf.) Ching	C.F. Zhao LZ12 (PE)	MW876326	Wei et al., 2021
Microsoroideae	***Lepisorus longifolius*** (Blume) Holttum	R. Wei SIWI4 (PE)	MW876327	Wei et al., 2021
Microsoroideae	***Lepisorus miyoshianus*** (Makino) Fraser-Jenk	X.C. Zhang 4511 (PE)	MW876328	Wei et al., 2021

(*continued on next page*)

Table 1 (*continued*)

Subfamily	Species	Voucher	GenBank ID	Cities
Microsoroideae	***Lepisorus ovatus*** (C. Presl) C.F. Zhao, R. Wei & X. C. Zhang	Cheng X. et al. FB209 (KUN)	MT130595	Du et al., 2021
Microsoroideae	***Lepisorus palmatopedatus*** (Baker) C.F. Zhao	FB663 (KUN)	MH707375	Du et al., 2019
Microsoroideae	***Lepisorus schraderi*** (Mett.) Ching	X.C. Zhang 9057 (PE)	MW876329	Wei et al., 2021
Microsoroideae	***Lepisorus spicatus*** (L.) L. Wang	R. Wei 29 (PE)	MW876330	Wei et al., 2021
Microsoroideae	***Lepisorus suboligolepidus*** Ching	Cheng X. et al. FB087 (KUN)	MT130652	Du et al., 2021
Microsoroideae	***Lepisorus superficialis*** (Blume) C.F. Zhao, R. Wei & X.C. Zhang	Cheng X. et al. FB071 (KUN)	MT130546	Du et al., 2021
Microsoroideae	***Lepisorus waltonii*** (Ching) S.L. Yu	C.F. Zhao NR6 (PE)	MK287776	Wang et al., 2019
Microsoroideae	***Leptochilus decurrens*** Blume	R. Wei WR0267 (PE)	MW876331	Wei et al., 2021
Microsoroideae	***Leptochilus ellipticus*** (Thunb.) Noot.	R. Wei WR0211 (PE)	MW876332	Wei et al., 2021
Microsoroideae	***Leptochilus ellipticus*** (Thunb.) Noot.	Cheng X. et al. FB212 (KUN)	MT130679	Du et al., 2021
Microsoroideae	***Leptochilus hemionitideus*** (C. Presl) Noot.	SS Liu 20,161,014 (SYS)	MH319943	Min et al., 2018
Microsoroideae	***Leptochilus henryi*** (Baker) X.C. Zhang	X.C. Zhang 7487 (PE)	MW876333	Wei et al., 2021
Microsoroideae	***Leptochilus macrophyllus*** (Blume) Noot.	R. Wei & al., 441 (PE)	MW876334	Wei et al., 2021
Microsoroideae	***Leptochilus pteropus*** (Blume) Fraser-Jenk.	R. Wei WR0281 (PE)	MW876341	Wei et al., 2021
Microsoroideae	***Microsorum insigne*** (Blume) Copel.	R. Wei & al., 440 (PE)	MW876340	Wei et al., 2021
Microsoroideae	***Microsorum punctatum*** (L.) Copel.	Mt. Shiwan Exp. 148 (PE)	MW876342	Wei et al., 2021
Microsoroideae	***Microsorum steerei*** (Harr.) Ching	R. Wei WR0620 (PE)	MW876343	Wei et al., 2021
Microsoroideae	***Phymatosorus cuspidatus*** (D. Don) Pic.Serm.	X.C. Zhang 4918 (PE)	MW876350	Wei et al., 2021
Microsoroideae	***Phymatosorus longissimus*** (Blume) Pic. Serm.	Cheng X. et al. FB042 (KUN)	MT130640	Du et al., 2021
Microsoroideae	***Thylacopteris papillosa*** (Blume) J.Sm.	R. Wei 345 (PE)	MW876376	Wei et al., 2021
Platycerioideae	***Hovenkampia schimperiana*** (Mett. ex Kuhn) Li Bing Zhang & X.M. Zhou	B. Liu CPG27233 (PE)	MW876325	Wei et al., 2021
Platycerioideae	***Platycerium bifurcatum*** (Cav.) C. Chr.	Cult. (FLBG)	MN623367	Liu et al., 2020
Platycerioideae	***Platycerium wallichii*** Hook.	L2691/CP06 (HITBC)	NC057599	Wang et al., 2021b
Platycerioideae	***Pyrrosia angustata*** (Sw.) Ching	Q. Wei wq004 (KUN)	MW876358	Wei et al., 2021
Platycerioideae	***Pyrrosia angustissima*** (Giesenh. ex Diels) C. M. Kuo	Unknown	MT210543	Unknown
Platycerioideae	***Pyrrosia assimilis*** (Baker) Ching	Unknown (IMPLAD)	MN617019	Yang et al., 2020a
Platycerioideae	***Pyrrosia bonii*** (Christ ex Gies.) Ching	SS Liu 201,615 (SYS)	NC040226	Cai et al., 2018
Platycerioideae	***Pyrrosia costata*** (Wall. ex C. Presl) Tagawa & K. Iwats.	Cheng X. et al. FB575 (KUN)	MT130646	Du et al., 2021
Platycerioideae	***Pyrrosia drakeana*** (Franch.) Ching	Unknown	MT210542	Unknown
Platycerioideae	***Pyrrosia heteractis*** (Mett. ex Kuhn) Ching	Cheng X. et al. FB171 (KUN)	MT130592	Du et al., 2021
Platycerioideae	***Pyrrosia lingua*** (Thunb.) Farwell	Unknown (IMPLAD)	MN885668	Yang et al., 2020b
Platycerioideae	***Pyrrosia penangiana*** (Hook.) Holttum	R. Wei 3014 (PE)	MW876359	Wei et al., 2021
Platycerioideae	***Pyrrosia petiolosa*** (Christ) Ching	Unknown (IMPLAD)	MN885667	Yang et al., 2020b
Platycerioideae	***Pyrrosia sheareri*** (Baker) Ching	Unknown (IMPLAD)	MN885669	Yang et al., 2020b
Platycerioideae	***Pyrrosia subfurfuracea*** (Hook.) Ching	SS Liu 201,620 (SYS)	NC047436	Min et al., 2019

(Jin et al., 2020). We set the number of rounds of extension to 25 and provided *Microsorum punctatum* (L.) Copel. (MW876342; Wei et al., 2021) plastome as the initial seed. Otherwise, all parameters were set to defaults. GFA and log files were examined to confirm the proper assembly of each plastome. To obtain accurate annotations, each species was annotated by PGA (Qu et al., 2019), CPGAVAS2 (Liu et al., 2012), and GeSeq (Tillich et al., 2017). All tRNAs were confirmed using tRNAscan-SE v2.0.7 (set Organellar tRNAs sequence source; Chan et al., 2019) by GeSeq. Positions of start and stop codons were manually verified in Geneious Prime 2019.2.1 when necessary. Circular genome maps were drawn with OmicsSuite v1.3.9 (Miao et al., 2023).

2.3. RNA extraction, sequencing, de novo assembly, and orthologs identification

The fresh leaves were collected from living plants and stored in liquid nitrogen. Total RNAs were isolated using the RNA plant Plus Reagent (Tiangen, Beijing, China). Library construction and sequencing were conducted by Biomaker Technology Co., Ltd. PE raw reads were obtained using the Illumina Nova6000 sequencing platform. Fastp was used to quality trim reads using the default parameters. The 6 Gb clean reads for each sample were *de novo* assembled using Trinity v2.8.5 (Grabherr et al., 2011). A Perl script (get_longest_isoform_seq_per_trinity_gene.pl) was used to retain the longest isoform from each gene. Minimap2 v2.17-r941 (Li, 2018) and Samtools v1.11 (Danecek et al., 2021) were chosen to filter out the organelle transcripts using the closest publicly available reference organelle genomes (chloroplast: *Microsorum punctatum* [MW876342; Wei et al., 2021]; mitochondrion: *Dryopteris crassirhizoma* Nakai [MW732172; Song et al., 2021]). CD-HIT-EST v4.8.1 (Li and Godzik, 2006) was implemented on the transcripts with a clustering threshold of 99%. Transdecoder v5.5.0 (Haas et al., 2013) was used to predict the coding regions of all the remaining transcripts and translate them into amino acids using default parameters.

Table 2
List of transcriptomes used in this study.

Subfamily	Species	Voucher	Location	Cities/SRA ID
Drynarioideae	***Selliguea feei*** Bory	xp755 (FUS)	Indonesia	SRR6920673
Microsoroideae	***Bosmania membranacea*** (D. Don) Testo	xp748 (FUS)	China	SRR6920666
Microsoroideae	***Goniophlebium niponicum*** (Mett.) Bedd.	RS-122 (CSH)	China	SRR2103725
Microsoroideae	***Goniophlebium niponicum*** (Mett.) Bedd.	xp723 (FUS)	China	SRR6920671
Microsoroideae	***Lecanopteris balgooyi*** Hennipman	JZW-AF7 (PYU, HITBC)	Indonesia (cult. XTBG, China)	This study
Microsoroideae	***Lecanopteris carnosa*** (Reinw.) Blume	JZW-AF19 (PYU, HITBC)	Indonesia (cult. XTBG, China)	This study
Microsoroideae	***Lecanopteris celebica*** Hennipman	JZW-AF18 (PYU, HITBC)	Indonesia (cult. XTBG, China)	This study
Microsoroideae	***Lecanopteris crustacea*** Copel. −1	JZW-AF1 (PYU, HITBC)	Indonesia (cult. XTBG, China)	This study
Microsoroideae	***Lecanopteris crustacea*** Copel. −2	JZW-AF2 (PYU, HITBC)	Indonesia (cult. XTBG, China)	This study
Microsoroideae	***Lecanopteris darnaedii*** Hennipman	JZW-AF12 (PYU, HITBC)	Indonesia (cult. XTBG, China)	This study
Microsoroideae	***Lecanopteris deparioides*** (Ces.) Baker −1	JZW-AF4 (PYU, HITBC)	Indonesia (cult. XTBG, China)	This study
Microsoroideae	***Lecanopteris deparioides*** (Ces.) Baker −2	JZW-AF5 (PYU, HITBC)	Indonesia (cult. XTBG, China)	This study
Microsoroideae	***Lecanopteris holttumii*** Hennipman	JZW-AF10 (PYU, HITBC)	Indonesia (cult. XTBG, China)	This study
Microsoroideae	***Lecanopteris lomarioides*** (Kunze ex Mett.) Copel.	JZW-AF21 (PYU, HITBC)	Indonesia (cult. XTBG, China)	This study
Microsoroideae	***Lecanopteris luzonensis*** Hennipman −1	JZW-AF9 (PYU, HITBC)	Philippines (cult. XTBG, China)	This study
Microsoroideae	***Lecanopteris luzonensis*** Hennipman −2	JZW-AF11 (PYU, HITBC)	cult. (XTBG, China)	This study
Microsoroideae	***Lecanopteris luzonensis*** Hennipman −3	JZW-AF22 (PYU, HITBC)	cult. (XTBG, China)	This study
Microsoroideae	***Lecanopteris mirabilis*** Copel. −1	JZW-AF3 (PYU, HITBC)	Indonesia (cult. XTBG, China)	This study
Microsoroideae	***Lecanopteris mirabilis*** Copel. −2	JZW-AF15 (PYU, HITBC)	Indonesia (cult. XTBG, China)	This study
Microsoroideae	***Lecanopteris pumila*** Blume ex Copel.	JZW-AF6 (PYU, HITBC)	Indonesia (cult. XTBG, China)	This study
Microsoroideae	***Lecanopteris sarcopus*** (Teijsm. & Binn.) Copel.	JZW-AF20 (PYU, HITBC)	Indonesia (cult. XTBG, China)	This study
Microsoroideae	***Lecanopteris sinuosa*** (Wall. ex Hook.) Copel. −1	JZW-AF14 (PYU, HITBC)	Indonesia (cult. XTBG, China)	This study
Microsoroideae	***Lecanopteris sinuosa*** (Wall. ex Hook.) Copel. −2	JZW-AF16 (PYU, HITBC)	cult. (XTBG, China)	This study
Microsoroideae	***Lecanopteris spinosa*** Jermy & T. Walker	JZW-AF8 (PYU, HITBC)	Indonesia (cult. XTBG, China)	This study
Microsoroideae	***Lecanopteris*** 'Tatsuta'	JZW-AF17 (PYU, HITBC)	cult. (XTBG, China)	This study
Microsoroideae	***Lecanopteris*** 'Yellow Tip'	JZW-AF13 (PYU, HITBC)	cult. (XTBG, China)	This study
Microsoroideae	***Lepisorus albertii*** (Regel) Ching	Zhangcf 3541 (FUS)	China	SRR6920665
Microsoroideae	***Lepisorus asterolepis*** (Baker) Ching	xp740 (FUS)	China	SRR6369205
Microsoroideae	***Leptochilus cantoniensis*** (Baker) Ching	xp741 (FUS)	China	SRR6369206
Microsoroideae	***Leptochilus ellipticus*** (Thunb.) Noot.	xp673 (FUS)	China	SRR6920667
Microsoroideae	***Microsorum punctatum*** (L.) Copel.	Cult. (KUKS)	Thailand	SRR8481129
Microsoroideae	***Microsorum scolopendria*** (Burm.) Copel.	xp696 (FUS)	China	SRR6920668
Platycerioideae	***Platycerium bifurcatum*** (Cav.) C. Chr.	RS-47 (CSH)	CSH	SRR2103728
Platycerioideae	***Platycerium elephantotis*** Schweinf.	K033766 (FUS)	KBCC	SRR6920672
Platycerioideae	***Pyrrosia subfurfuracea*** (Hook.) Ching	xp796 (FUS)	China	SRR6920669

OrthoFinder v2.3.8 (Emms and Kelly, 2019) was used to infer core-orthogroups based on all-against-all searches with default parameters, and only Single-Copy orthologous Genes (SCGs) present in all samples were selected for subsequent analyses. As a result, a total of 612 SCGs were used for downstream applications.

2.4. Dataset generation and phylogenetic inference

For the PT dataset, a Python script (get_annotated_regions_from_gb.py) was used to extract the sequences of each Protein-Coding Genes (PGGs) from the unaligned plastome of each taxon, as well as the Inter-Gene Spacer regions (IGSs). A total of 161 plastid loci shared among all samples were used for subsequent analyses. Each locus was aligned using the E-INS-I algorithm in Mafft v7.450 (Katoh and Standley, 2013) and trimmed with trimAl v1.3 with the option 'automated1' (Capella-Gutierrez et al., 2009). Subsequently, concatenation and Multi-Species Coalescent (MSC) methods were used to infer the plastome-based phylogenies. For the concatenation method, we used PhyloSuite v1.2.3 (Zhang et al., 2020) to concatenate the aligned loci using the plugin 'Concatenate Sequence'. ModelFinder (Kalyaanamoorthy et al., 2017) was employed to determine the best substitution model according to the Akaike Information Criterion (AICc). Maximum-Likelihood (ML) analyses were performed in IQ-tree v2.1.3 (Nguyen et al., 2015), with

support estimated using 5,000 replicates of the rapid bootstrapping algorithm. Bayesian Inference (BI) was constructed by Mrbayes v3.2.2 (Ronquist et al., 2012). Each Bayesian analysis comprised two independent runs of 2,000,000 generations from a random starting tree with one cold chain and three hot chains, and sampled the cold chain every 100 generations. Maximum Parsimony (MP) was constructed by PAUP* v4.0b10 (Swofford, 2002) with 1,000 bootstrap replicates using heuristic search. For the MSC method, recent studies have suggested that this method can yield a more accurate phylogenetic backbone when using plastid datasets (Gonçalves et al., 2019). The input ML single loci trees for Astral-II (Sayyari and Mirarab, 2016) were performed with IQ-tree with 1,000 rapid bootstrap replicates with the best-fitting substitution model for each locus chosen by ModelFinder. Finally, three concatenated trees and one coalescent tree were generated and visualized with their Maximum-Likelihood Bootstrap Support values (ML-BS), Bayesian Inference Posterior Probability (BI-PP), Maximum Parsimony Jackknife (MP-JK), and Astral Local Posterior Probabilities (AS-LPP) in Figtree v1.4.3 (Rambaut, 2017). For TT dataset, the software's Mafft and PAL2NAL v14.0 (Suyama et al., 2006) were used to align amino acid sequences with options '--localpair −-maxiterate 1000', and then converted the amino acid alignments to the corresponding codon alignments. Ambiguously aligned regions were excluded using trimAI with the '-automated1' command. Subsequently, concatenation and MSC methods were also used to infer the phylogenies as same mentioned above. In addition, we generated another two reduced datasets (PT_R and TT_R) after removing the two cultivated hybrids (*L.* 'Yellow Tip', and *L.* 'Tatsuta'). We re-infer 691 SCGs share with all samples for TT_R dataset. Phylogenetic trees were reconstructed using IQ-tree, MrBayes, PAUP, and Astral as described previously.

2.5. Estimation of DNA ploidy and genome size

Ploidy levels and absolute genome sizes of *Lecanopteris* s.s. species were estimated using flow cytometry. About 20–50 mg of fresh leaves was chopped with a razor blade in a plastic Petri dish containing 0.8 mL of ice-cold MG^b buffer (45 mM $MgCl_2{\cdot}6H_2O$, 20 mM MOPS, 30 mM $C_6H_5Na_3O_7$, 1 % (w/v) PVP 40, 0.2 % (v/v) Triton X-100, 10 mM Na_2EDTA, 20 μL/mL β-mercaptoethanol, pH 7.5). The crude suspension was filtered through a 40 μm nylon mesh to remove tissue debris, RNAase was added and the nuclei were then stained with Propidium Iodide (PI) (both at final concentrations of 50 μg/mL). Samples were stained for 30–60 min on ice. After incubation, each sample was run on a flow cytometer. DNA quantities were measured using a BD FACScalibur laser flow cytometer with Modifit v3.0. *Camellia sinensis* (L.) Kuntze 'Yunkang No. 10' (Genome Size = 3 Gb) and/or *Zea mays* L. (Genome Size = 2.3 Gb) were used as internal standard. DNA ploidy and absolute genome sizes were determined on the basis of the sample/standard ratio.

2.6. Detecting and visualizing gene tree discordance

To explore the discordance of *Lecanopteris* s.s. among gene trees, only one outgroup (*Bosmania membranacea* (D.Don) Testo) was included. Therefore, a total of 2,533 SCGs and 161 plastid loci shared with all samples were used for sequent analyses. We first employed Phyparts v0.0.1 (Smith et al., 2015) to calculate the conflict and concordance between gene trees and ML trees, which divides the nodes of gene trees into four situations: supporting the species tree topology, the main alternative topology, all other alternative topologies, and uninformative. We also used the Internode Certainty All (ICA; Salichos et al., 2014) values that resulted from Phyparts to quantify the degree of conflict on each node of a species tree given individual gene trees. ICA value ranges from −1 to 1. An ICA value close to 1 signifies robust agreement with the bipartition established by a specific internode, whereas an ICA value near 0 indicates comparable endorsement for one or more contradictory bipartitions. Conversely, negative ICA values imply that the targeted internode clashes with one or more bipartitions that are more prevalent, and ICA values approximating −1 denote a lack of backing for the bipartition delineated by a given internode. Furthermore, Quartet Sampling (Pease et al., 2018) was also employed to distinguish lack of support from conflicting support with 1,000 replicates based on the ML trees and the concatenated alignments. The QS method subsamples quartets from the input tree and alignment to assess the confidence, consistency, and informativeness of internal tree relationships, and the reliability of each terminal branch, and then four values are given in this analysis: QC = Quartet Concordance, QD = Quartet Differential, QI = Quartet Informativeness, and QF = Quartet Fidelity. The QC metric represents the ratio of concordant quartets to discordant quartets. A QC value approaching 1 signifies a prevalence of concordant quartets, while a value near 0 suggests an equal presence of concordant and discordant quartets, and a QC below 0 indicates a higher frequency of discordant quartets. QD assesses the sampling frequency of alternative relationships. Absence of QD implies no alternative topologies (equivalent to QC = 1). A QD value close to 1 indicates an equal occurrence of both alternative topologies, while a value near 0 indicates a preference for one of the alternatives. QI measures the proportion of replicates that provide informative data. A QI value of 1 indicates that all quartets are informative, whereas a value of 0 signifies uncertainty in all quartets. Phyparts results and Quartet Sampling results were visualized with phypartspiecharts.py (developed by Matt Johnson, available from: https://github.com/mossmatters/MJPythonNotebooks) and plot_QC_ggtree.R (created by Shui-Yin Liu, available from: https://github.com/ShuiyinLIU/QS_visualization).

2.7. ILS simulation and hybridization inference

To explore the possibility of hybridization or Incomplete Lineage Sorting (ILS) as a cause of discordance in *Lecanopteris* s.s., both TT and TT_R datasets were used for ILS simulation and hybridization inference. For ILS analyses, coalescent simulations were conducted to assess the potential of ILS as the sole factor contributing to discrepancies in gene trees. The population mutation parameter 'theta' associated with each internal branch was utilized to gauge the extent of ILS (high theta value means large ancestor population size and hence high ILS level), determined by comparing the ratio of branch length in mutation units estimated from IQ-tree to that in coalescent units estimated from Astral-II (Cai et al., 2020). We also simulated 20,000 gene trees under the MSC model with the R package Phybase v2.0 (the 'sim.coaltree.sp' function; Liu and Yu, 2010) and the Python package Dendropy v4.5.2 (the 'contained_coalescent_tree' function; Sukumaran and Holder, 2010) by using Astral tree as the guide tree, respectively. Subsequently, gene-tree quartet frequency analyses were conducted for each group of four taxon. Then we calculated all gene frequency of all four-taxon subsets within the simulated and observed gene tree datasets, and used the linear regression model 'lm ()' function in R to calculate correlations between them. Plots were made using ggplot2 v2.2.1 (Wickham, 2009).

Hyde v1.0.0 (Blischak et al., 2018) used a site-pattern probabilities method and conducted hypothesis testing using a Z-score, and phylogenetic invariants arising under the coalescent model with hybridization. The γ represents the likelihood of genetic inheritance from parent 1 (P1), while the complementary probability of the hybrid population being more closely related to parent 2 (P2) is denoted as 1-γ. Notably, substantial γ values approximating 0.5 typically suggest a recent occurrence of hybridization, while values close to 0 or 1 are indicative of ancient hybridization events persisting in present-day species. The γ threshold was established at 0.3 and 0.7 (Liu et al., 2022; Nie et al., 2023). Besides, PhyloNet v3.8.0 (Than et al., 2008) was used to reconstruct phylogenetic networks from gene trees under a maximum pseudo-likelihood (InferNetwork_MPL; Yu and Nakhleh, 2015) based on the multi-individual dataset. Due to computational restrictions, a maximum of five reticulation events was set and run with 10 runs to ensure accuracy. Furthermore, the command 'CalGTProb' (Yu et al., 2012) was used to compute the likelihood scores. The phylogenetic networks were visualized in Dendroscope v3.8.1 (Huson and Scornavacca, 2012). We

then employed QuIBL (Edelman et al., 2019), a new tree-based method, to differentiate between the models with ILS + introgression and with ILS only, and to obtain localized information on introgression.

2.8. Age estimation and biogeography

Penalized likelihood (PL) dating analysis was conducted using treePL v2.6.3 (Smith and O'Meara, 2012) based on the PT and TT datasets. Due to the lack of fossil records of *Lecanopteris* s.s., we selected a leaf fossil record of *Protodrynaria takhtajanii* Vikulin & A. Bobr (33.9 Ma–66 Ma; Vikulin and Bobrov, 1987; Van Uffelen, 1991) as a calibration to constrain the stem age of Drynarioideae for the dating analysis. The fossil record was used widely in previous molecular dating analyses (e.g., Testo and Sundue, 2016; Qi et al., 2018; Du et al., 2021; Pelosi et al., 2022). Following the guidelines of Maurin (Maurin, 2020), 1,000 bootstrap replicates using the best ML tree as a topology constraint were conducted in IQ-tree. Then, a cross-validation process for the ML tree was performed with rate-smoothing values ranging from 10^{10} to 10^{-30} and a 'cvmultstep' of 0.1 to determine the appropriate smoothing value (1e-07 for plastome data, and 1e-10 for transcriptome data). Lastly, TreeAnnotater v2.6.3 (Drummond et al., 2012) was employed to summarize all dated 1000 bootstrap replicates into a maximum clade credibility (MCC) tree. The resulting MCC tree was visualized using Figtree.

For biogeographical analysis, the R package 'BioGeoBEARS' (Matzke, 2018) implemented in RASP v4.4 (Yu et al., 2020) was used to estimate ancestral ranges for taxa in the dated phylogenies. Six biogeographical regions were defined (refer to Woodruff, 2010; Lohman et al., 2011; Cox et al., 2016; Kooyman et al., 2019; Husson et al., 2019; Meng and Song, 2023): (A) continental Asia/East Asia (including Indochina and continental Asia); (B) Sundaic region (including Ball Island, Borneo, Malaya, Java, and Sumatra); (C) Philippines (including Philippines and Palawan); (D) Wallacea (including Sulawesi, Lombok Island, and Maluku), and (E) Sahul shelf (including New Guinea and Australia). The six areas were chosen to best represent the current global distribution of the genus *Lecanopteris* s.s. and to detect past major biogeographical shifts within the genus. Distribution data for *Lecanopteris* s.s. were mainly followed digital images via Jstor (https://plants.jstor.org/), Global Biodiversity Information Facility (https://www.gbif.org/), and referred to other literature (e.g., Gay et al., 1994). The MCC tree was used as input tree file of RASP. We first used the R package 'BioGeoBEARS' to select the historical biogeography model: DEC (dispersal extinction cladogenesis; Ree and Smith, 2008); DIVALIKE (a likelihood-based implementation of dispersal vicariance analysis; Ronquist, 1997); and BAYAREALIKE (a likelihood implementation of BayArea; Landis et al., 2013). Furthermore, we specifically tested models that incorporate the parameter 'jump' (J) for each method. A dispersal multiplier matrix was specified following the definition of Buerki et al. (2011): low dispersal = 0.01; medium dispersal = 0.5; high dispersal = 1.0 (Table S1), and analyses were carried out with a distance matrix. These models assume speciation events at the nodes of the phylogeny, with one daughter lineage retaining the ancestral range and the other lineage occupying a new range (Matzke, 2014). The most fitted model was selected using AIC value corrected for sample size (AICc) and its weight (wt). The number of maximum ranges was constrained to six to avoid underestimating vicariance events. After providing a biogeographical model, we also estimated the number and type of biogeographic events in RASP, the stochastic mapping algorithm generates simulations across nodes and branches of the provided phylogeny, including locations of all events along the branches in that simulation.

3. Results

3.1. Characteristics of the chloroplast genomes

Of the 22 generated genome skimming data, we generated PE raw reads ranging from 12,122,358 reads for *Lecanopteris deparioides* −1 to 15,269,990 reads for *L. balgooyi*, respectively (Table S2). After data quality filtering, we finally retained a total of 12,122,352–15,269,986 reads of the clean data, and the percentage of GC content ranged from 37.89 % to 38.95 % (Table S2). All of the chloroplast genomes were composed of a single circular double-stranded DNA molecule, and displayed the typical quadripartite structure, consisting of a pair of Inverted Repeats (termed IRA and IRB), separated by the Large Single Copy regions (LSC) and Small Single Copy regions (SSC) (Fig. 1). The plastomes of the different *Lecanopteris* s.s. species showed variation in size and GC content (Fig. 1; Table 3). The plastome sizes ranged from 151,170 bp in *L. mirabilis* −1 of the crustacea group to 187,319 bp in *L. carnosa* of the pumila group. We observed only marginal variation in the LSC, ranging from 79,276 bp in *L. lomarioides* of the crustacea group to 79,822 bp in *L. mirabilis* −2 of the crustacea group (Table 3). Substantial length variation was evident in the SSC and IR (Table 3). The SSC length ranged from 119 bp in *L. deparioides* −2 to 21,607 bp of the pumila group in *L. lomarioides* of the crustacea group (Table 3). The IR ranged from 24,905 bp in *L. mirabilis* −1 of the crustacea group to 53,891 bp in *L. carnosa* of the pumila group (Table 3). The overall GC content ranged narrowly from 39.70 % to 41.30 %, whereas the GC content in the LSC, SSC, and IR regions were 38.50–38.90 %, 20.10–40.60 %, and 40.60–46.20 % (Table 3), respectively. In short, we found that the plastomes of *Lecanopteris* s.s. can be divided into two types: the crustacea group type (Fig. 1a) and the pumila group + the darnaedii group type (Fig. 1b). The crustacea group type typically has the smallest plastome size and IR size, as well as the largest SSC size, plastome GC content, LSC GC content, SSC GC content, and IR GC content (Table 3). In turn, the pumila group + the darnaedii group type has the smallest SSC size, plastome GC content, LSC GC content, SSC GC content, and IR GC content, as well as the largest plastome size and IR size (Table 3).

The protein-coding genes, rRNA genes, tRNA genes, and intron numbers varied in each lineage (Fig. 1). The plastomes of all eight accessions of the crustacea group, encoded an identical set of 128 genes with 13 being duplicated in the IR regions. Among the 128 genes, there were 89 protein-coding genes, 31 tRNA genes, and eight rRNA genes (Fig. 1a). Species of the pumila group and the darnaedii group also often shared the same structure and approximately the same gene and intron contents. However, each plastome contained 145 genes with 30 being duplicated in the IR regions (Fig. 1b). In addition, each plastome contained 104 protein-coding genes, 33 tRNA genes, and eight rRNA genes. However, it is worth mentioning that all species of *Lecanopteris* s.s. always share with same features (Fig. 1). For instance, (1) all samples contained 115 unique genes, and among the 115 unique genes, there were 85 protein-coding genes, 26 tRNA genes, and four rRNA genes. (2) The 5-end exon of the *rps*12 gene was located in the LSC region, and the intron and 3-end exon of the gene were situated in the IR region; (3) four tRNA genes (*trn*A, *trn*G, *trn*I, and *trn*L) and nine protein-coding genes (*atp*F, *ndh*A, *ndh*B, *pet*B, *pet*D, *rpl*2, *rpl*16, *rpo*C1, and *rps*16) contained a single intron, and three genes including *rps*12, *clp*P, and *ycf*3 contained two introns.

3.2. Phylogenetic relationships

The PT and PT_R datasets were 111,231 and 106,309 nucleotides in length, respectively. And both datasets were identified GTR + F + I + G4 as the best model of evolution (Table S3). The four phylogenetic analyses (MP, ML, BI, and AS) revealed generally congruent topologies. The TT dataset included 35 samples with 804,963 nucleotide sites, 177,509 sites are parsimony-informative, and 521,938 sites are invariant. The

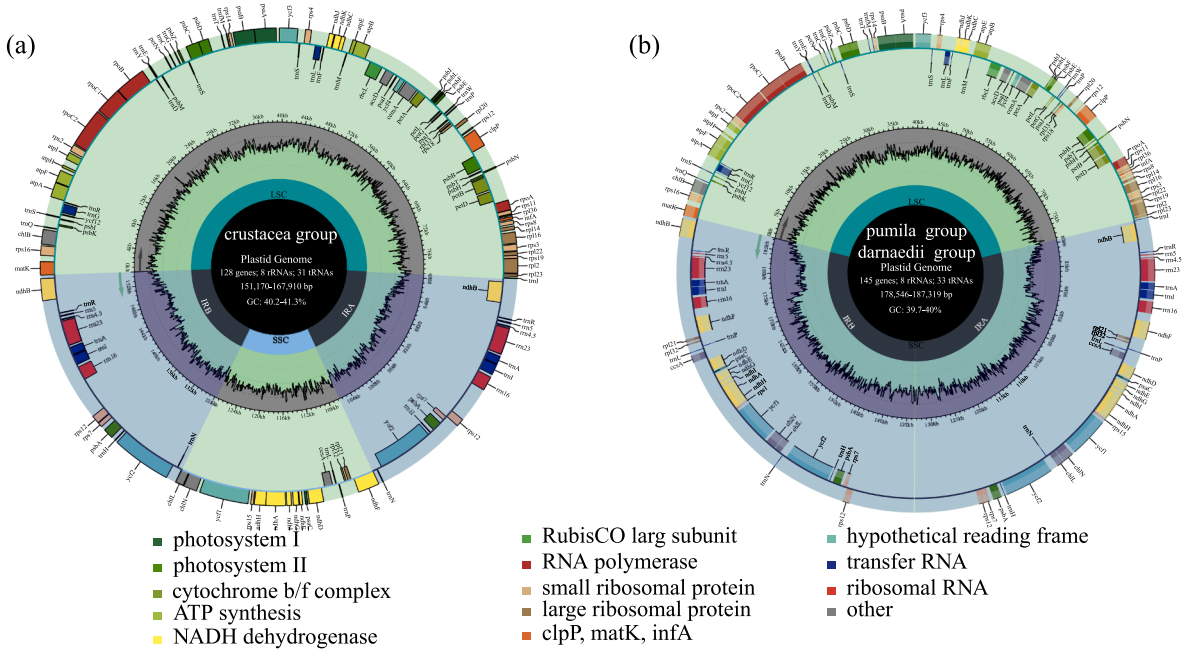

Fig. 1. The plastome maps of *Lecanopteris* s.s.. a, the crustacea group plastomes map. b, the darnaedii group and the pumila group plastomes map. The dark grey track inside the map shows the GC content. Genes on the outside of the map are transcribed clockwise, and genes on the inside are transcribed counterclockwise. Genes belonging to different functional groups are shown in different colours; see the legend for groups.

Table 3
General characteristics of *Lecanopteris* s.s. plastid genomes.

Species	Plastome Size (bp)	Plastome GC content (%)	LSC Size (bp)	LSC GC content (%)	SSC Size (bp)	SSC GC content (%)	IR Size (bp)	IR GC content (%)
Lecanopteris balgooyi Hennipman	186,438	39.9	79,415	38.5	139	20.1	53,442	40.9
Lecanopteris carnosa (Reinw.) Blume	187,319	40	79,400	38.7	137	30.7	53,891	41.1
Lecanopteris celebica Hennipman	186,783	40	79,414	38.7	137	31.4	53,616	41
Lecanopteris crustacea Copel. −1	154,426	40.5	79,344	38.9	21,548	35.4	26,767	44.9
Lecanopteris crustacea Copel. −2	154,424	40.5	79,344	38.9	21,548	35.4	26,766	44.9
Lecanopteris darnaedii Hennipman	179,567	39.7	79,452	38.6	191	38.7	49,962	40.6
Lecanopteris deparioides (Ces.) Baker −1	185,945	40	79,352	38.7	119	27.7	53,237	41
Lecanopteris deparioides (Ces.) Baker −2	185,946	40	79,351	38.7	119	27.7	53,238	41
Lecanopteris holttumii Hennipman	179,465	39.7	79,456	38.6	187	36.9	49,911	40.6
Lecanopteris lomarioides (Kunze ex Mett.) Copel.	157,373	40.7	79,276	38.9	21,607	35.3	28,245	45.3
Lecanopteris luzonensis Hennipman −1	178,617	39.7	79,407	38.7	234	31.6	49,488	40.6
Lecanopteris luzonensis Hennipman −2	178,553	39.7	79,399	38.7	170	28.2	49,492	40.6
Lecanopteris luzonensis Hennipman −3	178,625	39.7	79,409	38.7	234	31.6	49,491	40.6
Lecanopteris mirabilis Copel. −1	151,170	40.2	79,821	38.8	21,539	35.6	24,905	44.5
Lecanopteris mirabilis Copel. −2	151,175	40.2	79,822	38.8	21,539	35.6	24,907	44.5
Lecanopteris pumila Blume ex Copel.	182,298	39.9	79,400	38.7	166	41.6	51,366	40.9
Lecanopteris sarcopus (Teijsm. & Binn.) Copel.	156,041	40.7	79,371	38.9	21,604	35.5	27,533	45.4
Lecanopteris sinuosa (Wall. ex Hook.) Copel. −1	167,910	41.3	79,407	38.9	21,583	35.4	33,460	46.2
Lecanopteris sinuosa (Wall. ex Hook.) Copel. −2	166,240	41.1	79,431	38.8	21,589	35.4	32,610	45.8
Lecanopteris spinosa Jermy & T. Walker	179,232	39.7	79,369	38.5	163	33.1	49,850	40.6
Lecanopteris 'Tatsuta'	178,546	39.7	79,402	38.7	170	29.4	49,487	40.6
Lecanopteris 'Yellow Tip'	178,603	39.7	79,449	38.7	170	28.2	49,492	40.6

TT_R dataset included 33 samples with 826,069 nucleotide sites, 180,988 sites are parsimony-informative, and 539,120 sites are invariant. GTR F + I + G4 was identified as the best model of evolution for SCGs (Table S3). MP, ML, BI, and AS all produced a fully resolved topology. Due to the absence of the closet genera of *Dendroconche* and *Zealandia*, the monophyly of *Lecanopteris* s.s. was supported (ML-BS = 100, MP-JK = 100, BI-PP = 1.0, AS-LPP = 1.0; Figs. 2 and 3, Fig. S1 and S2), but need further investigation. Besides, almost all major genera within the phylogeny were highly supported.

3.2.1. Plastome analysis

For the PT and PT_R datasets, except for the darnaedii group, both the pumila group and the crustacea group were not recovered as monophyletic (Fig. 2, Fig. S1). As a general result, the crustacea group, sister to all the species classically included in the other two groups with high statistical values (Fig. 2, Fig. S1).

Three clades can be recognized within the crustacea group. First, the *Lecanopteris mirabilis* lineage, which contained the single species *L. mirabilis* (Fig. 2, Fig. S1). The second clade, supported by full support, also comprises one species *L. sinuosa* (Fig. 2, Fig. S1). The rest of the species of crustacea group form another large clade: *L. crustacea* clade (Fig. 2, Fig. S1). Within it, one is the *L. crustacea* subclade. The other subclade is the *L. lomarioides* lineage, which comprises two species, *L. lomarioides* and *L. sarcopus*. The pumila group can be divided into five clades: *L. pumila* clade, *L. luzonensis* clade, *L. balgooyi* clade, *L. deparioides* clade, and *L. carnosa* clade (Fig. 2, Fig. S1). Except *L. carnosa* clade contained two species (*L. carnosa* and *L. celebica*), the remaining clades each contained only one species (Fig. 2, Fig. S1). Besides, *L. luzonensis* forms two independent branches (Fig. 2, Fig. S1), two horticultural varieties (*L.* 'Yellow Tip' and *L.* 'Tatsuta') with one of the accessions of *L. luzonensis* form sister relationship (Fig. 2). The darnaedii group was recovered as the sister to the *L. balgooyi* clade + *L. deparioides* clade + *L. carnosa* clade, and *L. spinosa* sister to *L. holttumii* and *L. darnaedii* (Fig. 2, Fig. S1).

3.2.2. Nuclear analysis

The TT and TT_R datasets largely agree with the plastome-based results in recovering the paraphyly of the pumila group and the crustacea group in all of the resulting phylogenies (Fig. 3, Fig. S2). Except for coalescent analyses (available at: https://doi.org/10.6084/m9.figsh

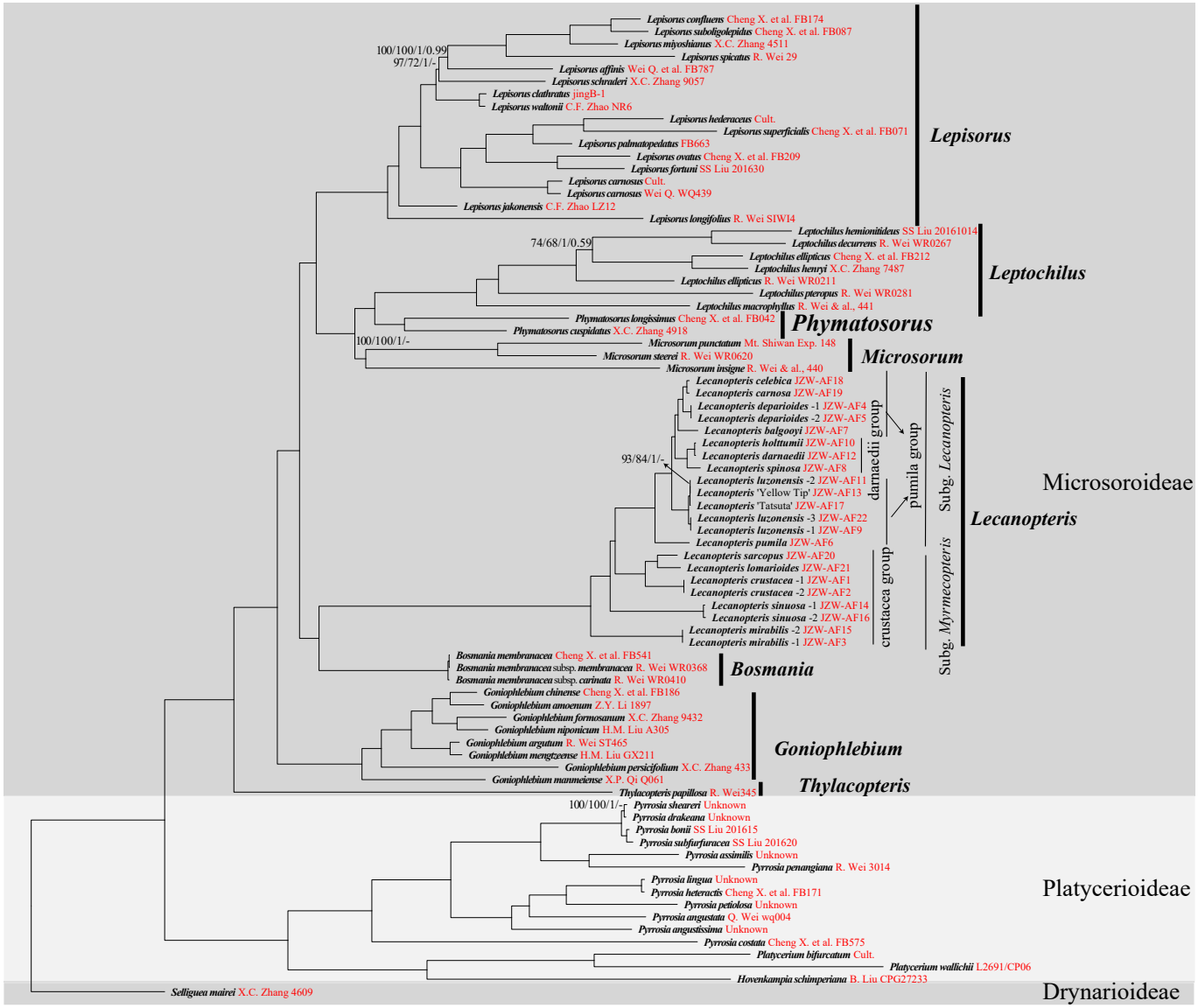

Fig. 2. Maximum likelihood phylogeny of *Lecanopteris* s.s. inferred from IQ-tree analysis of the PT data. The numbers above the branches represent ML-BS/MP-JK/BI-PP/AS-LPP. Values of 100 or 1.00 are not displayed. Voucher information is indicated in red. (For interpretation of the references to colour in this figure legend, the reader is referred to the web version of this article.)

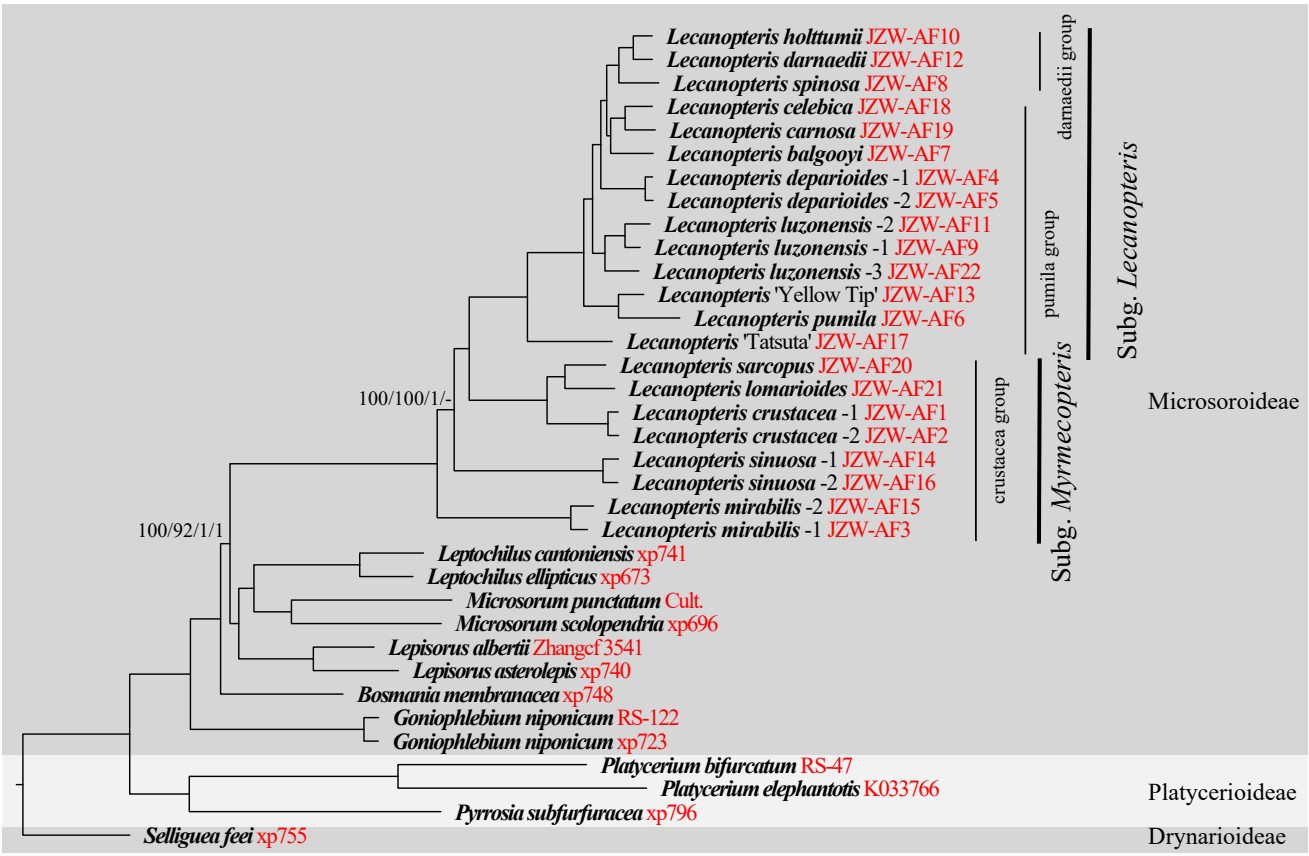

Fig. 3. Phylogenetic tree reconstruction using maximum likelihood (ML) based on TT data. Numbers above the branches represent ML-BS/MP-JK/BI-PP/AS-LPP. Values of 100 or 1.00 are not displayed. Voucher information is indicated in red. (For interpretation of the references to colour in this figure legend, the reader is referred to the web version of this article.)

are.25309648), the concatenation (ML, MP, and BI) analyses based on TT dataset yielded almost identical topologies, and most of the deeper nodes received full support in terms of ML-BS, MP-JK, BI-PP (Fig. 3, Fig. S2). The crustacea group was also divided into three clades: *Lecanopteris mirabilis* clade, *L. sinuosa* clade, and the *L. crustacea* clade. *L. mirabilis* clade as the first divergence clade of *Lecanopteris* s.s., and then *L. sinuosa* clade, *L. crustacea* clade divergence in turn with full support (ML-BS = 100, MP-JK = 100, BI-PP = 1.0; Fig. 3, Fig. S2). However, phylogenetic trees based on TT_R dataset (Fig. S2) and coalescent analysis based on TT dataset (available at: https://doi.org/10.6084/m9.figshare.25309648) recovered *L. sinuosa* clade sister to the *L. crustacea* clade with full support (AS-LPP = 1.0). The pumila group can be divided into six clades based on TT dataset: *L.* 'Tatsuta' clade, *L. pumila* clade, *L. luzonensis* clade, *L. balgooyi* clade, *L. deparioides* clade, and *L. carnosa* clade (Fig. 3). *L.* 'Tatsuta' clade contained one horticultural variety (*L.* 'Tatsuta') and is sister to all species of *Lecanopteris* s.s. except the crustacea group (Fig. 3). *L.* 'Yellow Tip' with *L. pumila* form sister relationship and an independent clade (Fig. 3). Three accessions of *L. luzonensis* form a clade (Fig. 3, Fig. S2). The darnaedii group were recovered as a monophyletic lineage and sister to the *L. balgooyi* clade with full support (ML-BS = 100, MP-JK = 100, BI-PP = 1.0; Fig. 3, Fig. S2).

3.3. Cytotypes

The results obtained from flow cytometry revealed that *Lecanopteris* s.s. only has two cytotypes but a wide range in genome sizes (Table 4). The genome size ranged from 8.24 Gb in *L. luzonensis* −2 to 42.50 Gb in *L. mirabilis* −2 (Table 4). The DNA amount of *L. carnosa* and *L. sarcopus* was estimated to be 12.47–12.87 Gb and 12.78–13.11 Gb by using different internal standard (*Camellia sinensis* or *Zea mays*), respectively (Table 4). Except for three samples of *L. luzonensis* with different genome size (8.24–12.38 Gb), there is little variation in genome size among different materials of the same species (Table 4). Although flow cytometry results were not supplemented by conventional chromosome counts to confirm the ploidy level, we found a nearly fourfold change in genome size. The genome size of *L. mirabilis* was 42.03 ± 0.47 Gb, which is four times larger than others and is recognized as an octoploid, all the remaining species of *Lecanopteris* s.s. were recognized as diploid, and the genome size was estimated to be 12.65 ± 4.41 Gb (Table 4).

3.4. Topological conflicts

Although the phylogenetic relationships among *Lecanopteris* s.s. received strong to full support (Figs. 2 and 3, Fig. S1 and S2), the conflict analyses of Phyparts and QS detected disagreements among individual loci between the PT and TT datasets (Fig. 4). In summary, the Phyparts result and the QS result demonstrated that the interspecies relationships based on plastid genes were confirmed with higher ICA values and QS support than the conflicts result based on nuclear genes.

Within *Lecanopteris* s.s., *L. mirabilis* as the first divergence lineage of *Lecanopteris* s.s. was supported by 160 informative plastid gene trees and 2,533 informative nuclear gene trees (ICA = 1) and had full QS support (1/–/1) (Fig. 5). *L. sinuosa* as the second lineage was supported by 844 nuclear genes (out of 2,533; ICA = 0.47) and full QS support (1/–/1) in nuclear dataset (Fig. 4b). However, *L. sinuosa* as the second lineage was supported by 88 plastid genes (out of 160; ICA = 0.25) and strong QS support (0.93/0/0.99). *L. carnosa* + *L. lomarioides* + *L. sarcopus* as the third lineage of *Lecanopteris* s.s. was supported by only 56 plastid genes (out of 160; ICA = 0.13) and 614 nuclear genes (out of 2,533; ICA=0.42)

Table 4
Summary of the flow cytometer results.

Species	Internal standard	Internal reference fluorescence intensity	Fluorescence intensity of the sample to be tested	Ratio	Genome (Gb)
Lecanopteris crustacea Copel. −1	***Camellia sinensis***	23.93	105.28	4.40	13.20
Lecanopteris crustacea Copel. −2	***Camellia sinensis***	21.42	89.65	4.19	12.56
Lecanopteris mirabilis Copel. −1	***Camellia sinensis***	34.87	483.04	13.85	41.56
Lecanopteris deparioides (Ces.) Baker −1	***Camellia sinensis***	30.84	106.06	3.44	10.32
Lecanopteris deparioides (Ces.) Baker −2	***Camellia sinensis***	30.67	103.01	3.36	10.08
Lecanopteris pumila Blume ex Copel.	***Camellia sinensis***	29.27	144.01	4.92	14.76
Lecanopteris balgooyi Hennipman	***Camellia sinensis***	31.18	149.2	4.79	14.36
Lecanopteris spinosa Jermy & T. Walker	***Camellia sinensis***	21.44	90.06	4.20	12.60
Lecanopteris luzonensis Hennipman −1	***Camellia sinensis***	21.89	89.88	4.11	12.32
Lecanopteris holttumii Hennipman	***Camellia sinensis***	22.11	90.28	4.08	12.25
Lecanopteris luzonensis Hennipman −2	***Camellia sinensis***	33.55	92.16	2.75	8.24
Lecanopteris darnaedii Hennipman	***Camellia sinensis***	31.68	154.73	4.88	14.65
Lecanopteris 'Yellow Tip'	***Camellia sinensis***	22.2	90.67	4.08	12.25
Lecanopteris sinuosa (Wall. ex Hook.) Copel. −1	***Camellia sinensis***	22.34	90.19	4.04	12.11
Lecanopteris mirabilis Copel. −2	***Camellia sinensis***	33.31	471.89	14.17	42.50
Lecanopteris sinuosa (Wall. ex Hook.) Copel. −2	***Camellia sinensis***	39.77	190.71	4.80	14.39
Lecanopteris 'Tatsuta'	***Camellia sinensis***	38.22	184.87	4.84	14.51
Lecanopteris celebica Hennipman	***Camellia sinensis***	13.35	53.42	4.00	12.00
Lecanopteris carnosa (Reinw.) Blume	***Camellia sinensis***	21.01	90.12	4.29	12.87
Lecanopteris carnosa (Reinw.) Blume	***Zea mays***	16.88	91.49	5.42	12.47
Lecanopteris sarcopus (Teijsm. & Binn.) Copel.	***Camellia sinensis***	20.5	89.57	4.37	13.11
Lecanopteris sarcopus (Teijsm. & Binn.) Copel.	***Zea mays***	15.82	87.89	5.56	12.78
Lecanopteris lomarioides (Kunze ex Mett.) Copel.	***Camellia sinensis***	40.54	190.78	4.71	14.12
Lecanopteris luzonensis Hennipman −3	***Camellia sinensis***	43.79	180.68	4.13	12.38

(Fig. 4b). Although the third clade of *Lecanopteris* s.s. had full QS support (1/–/1) based on plastid genes, the node relationship was confirmed with a higher frequency of discordant quartets (QC=-0.63), a preference for one of the alternatives (QD = 0), and all quartets were informative (QI = 1) (Fig. 4a). *L. pumila* as the first divergence clade of the pumila group and the darnaedii group was supported by 116 plastid genes (out of 160; ICA = 0.16) and full QS support (1/–/1) (Fig. 4a). In contrast, the *L.* 'Tatsuta' clade as the first divergence clade of the pumila group and the darnaedii group was supported by 1141 nuclear genes (out of 2,533; ICA = -0.51), and this node was supported by 0.43 % of informative quartets (QC = 0.0043) with a preference for one of the alternatives (QD = 0) and 100 % out of quartets being informative (QI=1) (Fig. 4b). *L.* 'Yellow Tip' sister to *L. luzonensis* −2 and together a sister to *L.* 'Tatsuta' was supported by 51 plastid genes (out of 160; ICA = 0.15) and 38 plastid genes (out of 160; ICA = -0.13), respectively (Fig. 4a). The sister relationship of *L. pumila* and *L.* 'Yellow Tip' was supported by 1,328 nuclear genes (out of 2533; ICA = 0.36) and moderate QS support, with a signal of a possible alternative topology (0.59/0/1) (Fig. 4b). The darnaedii group was sister to *L. balgooyi* supported by only 204 nuclear genes (out of 2,533; ICA = -0.21; QS -0.055/0/1) (Fig. 4b). Meanwhile, the sister relationship of the darnaedii group and *L. balgooyi* + *L. deparioides* + *L. carnosa* + *L. celebica* also supported by only 45 plastid genes (out of 160; ICA = 0.05), but had full QS support (1/–/1) (Fig. 4a).

3.5. Simulations of ILS, network analysis, and gene flow

For the ILS analysis, the theta values were found range from 0.003 to 0.029 based on TT dataset, and the ancestor branches of the pumila group and the darnaedii group showed the highest level of ILS, while the other ancestor branches of the species of *Lecanopteris* s.s. showed a relatively lower level of ILS (Fig. 5a). However, the theta values were found ranged from 0.003 to 0.015 after removing the two cultivated hybrids (Fig. S3). Besides, the 20,000 gene trees were further simulated with the ILS conditions by Phybase (Fig. 5c, Fig. S3c) and Dendropy (Fig. 5d, Fig. S3d) under the multispecies coalescent model. There were found a low correlation based on TT dataset between the observed gene trees and simulated ones (R^2 = 0.66 or 0.92) (Fig. 5c-d), but had high correlation based on TT_R dataset between the observed gene trees and simulated ones (R^2 = 0.94 or 0.99) (Fig. S3c-d). Furthermore, the QuIBL analysis revealed that only 49.2 % (2,274 triplets) of the tested triplets (4,620 triplets) and 47.5 % (1,626 triplets) of the tested triplets (3,420 triplets) showed significant evidence for ILS based on different SCGs

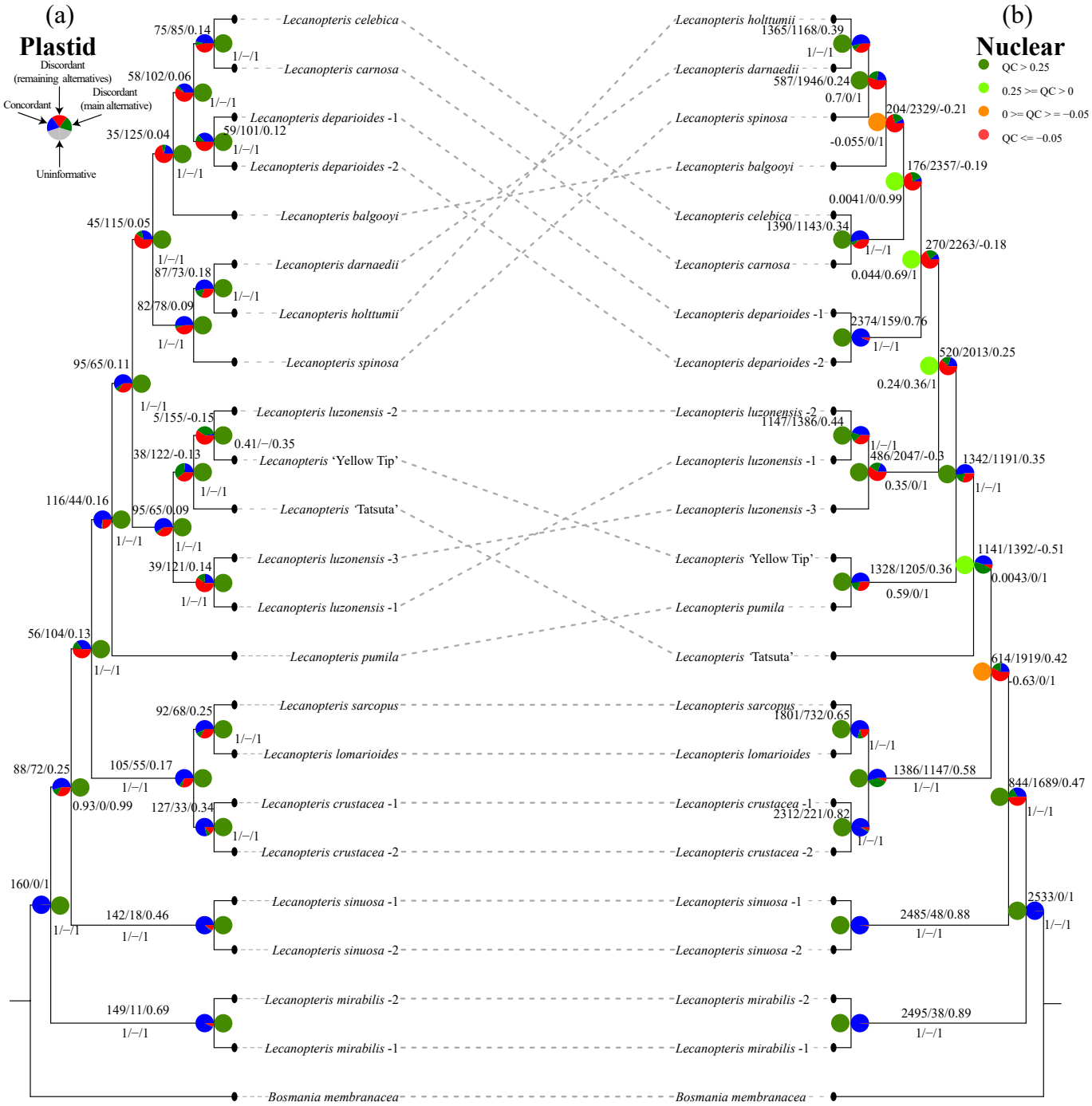

Fig. 4. The tanglegram phylogenies showing cytonuclear discordance between plastid (a) and nuclear (b). Numbers above the nodes show the number of concordant loci the total number of conflicting loci (support main alternative + support remaining alternatives), and the Internode Certainty All (ICA). The numbers below branches indicate the Quartet sampling internal node score (Quartet concordance/Quartet differential/Quartet informativeness).

dataset (Tables S4 and S5; Fig. 5e, Fig. S3e).

For the hybridization inference, the QuIBL analysis suggests that 50.8 % (2,346) triplets based on TT dataset and 52.5 % (1,794) triplets based on TT_R dataset showed significant levels of introgression (ΔBIC>10) (Tables S4 and S5; Fig. 5e, Fig. S3e). Additionally, all the results of QuIBL were further divided into 231 or 190 species pairs and calculated the average of the total introgression proportion (total-IntroProp.avg) for each species pair (Tables S4 and S5; Fig. 5e, Fig. S3e). Most high value results were found in the pumila group and the darnaedii group (Tables S4 and S5; Fig. 5e, Fig. S3e). We also used the filtered HyDe results for detecting hybridization events. A total of 694 out of 4,620 hypotheses based on TT dataset and 475 out of 3,420 hypotheses based on TT_R dataset tested by HyDe showed significant evidence of a hybridization event (Tables S6 and S7). The γ value for 503 out of the 694 hypotheses based on TT dataset and 371 out of 475 hypotheses based on TT_R dataset were greater than 0.7 and less than 0.3, indicating ancient hybridization events, and only 191 or 104 γ values were close to 0.5 ($0.3 < \gamma < 0.7$), suggesting recent hybridization events (Tables S6 and S7). Up to five hybridization events among the clades of *Lecanopteris* s.s. were examined in PhyloNet (Fig. 5f-k, Fig. S3f-k). A plot of log pseudolikelihood scores suggested that the best network allowed four hybridization events (Fig. 5f, S3f). One reticulation event, in which

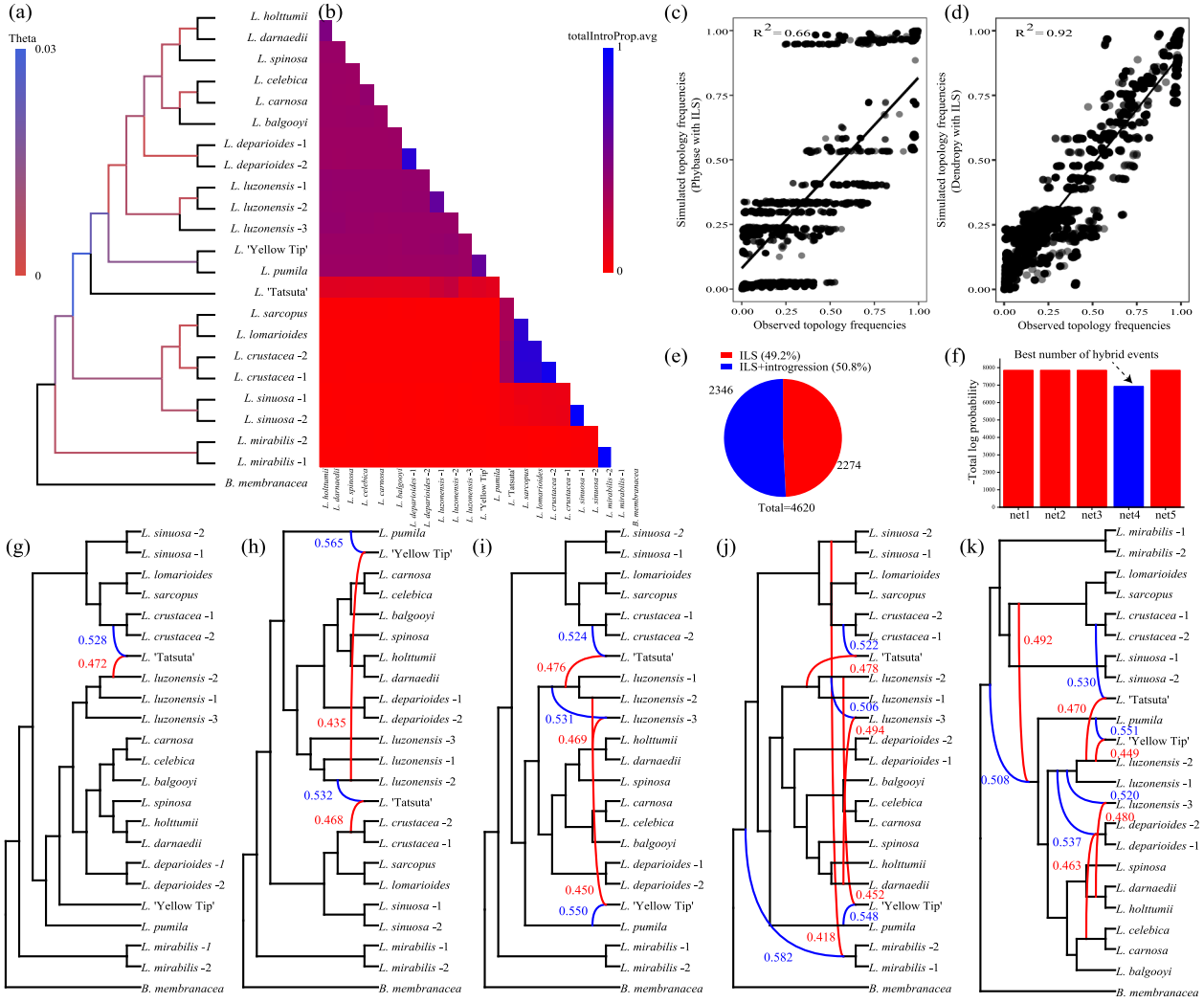

Fig. 5. ILS and gene flow analysis based on TT dataset. a, Estimated theta value for each internal branch; b, the average totalIntroProp per species pair inferred through the QuIBL analysis; c, correlation analyses of topology frequency of the simulation with ILS by DendroPy and empirical observation; d, correlation analyses of topology frequency of the simulation with ILS by Phybase and empirical observation; e, the triplet ratio of different models from QuIBL result; f, the total log probability of one to five maximum number of reticulations; g, species network inferred from PhyloNet pseudolikelihood analyses with one to five hybridization events, The major and minor edges of hybrid nodes are shown as blue and red curved lines (edges with an inheritance contribution), respectively. (For interpretation of the references to colour in this figure legend, the reader is referred to the web version of this article.)

gene flow from *L. luzonensis* and the ancestors of *L. crustacea* was detected in all five examinations based on TT dataset (Fig. 5g-k), with *L.* 'Tatsuta' had an inheritance probability of 0.522 to 0.532 from ancestors of *L. crustacea* and an inheritance probability of 0.478 to 0.488 from *L. luzonensis*. *L.* 'Yellow Tip' as a hybrid was inferred in four examinations based on TT dataset (Fig. 5h-k), with an inheritance probability of 0.548–0.565 from the *L. pumila* lineage and 0.435–0.452 from the *L. luzonensis* lineage. *L. luzonensis* −3 also had been detected gene flow from the *L. luzonensis* lineage and the *L. darnaedii* + *L. holttumii* lineage in three examinations based on TT dataset (Fig. 5i-k) and in all five examinations based on TT_R dataset (Fig. S3i-k). For the reticulation event of *L. deparioides*, *L. mirabilis*, and the ancestor of *L. carnosa* + *L. celebica*, each had detected the gene flow (Fig. 5j-k, S3g-k).

3.6. Biogeography

The chronograms constraining the stem node of Drynarioideae inferred by treePL from both plastid and nuclear are shown in Fig. 6 and Fig. 7. In addition, each was summarized with the ancestral range estimated by BioGeoBEARS. Among the three biogeographic models tested, the BAYAREALIKE+J model was determined as the best-fit model for both plastid and nuclear sequences, because it yielded the lowest AIC value and the highest AICc_wt (Table S8).

3.6.1. Plastid biogeography

The estimated age for the split between Platycerioideae and Microsoroideae was around the Paleocene–Eocene boundary (node 152; 95% highest posterior density (HPD) = 50.59–55.78 Ma), and both subfamilies were inferred to have originated in Continental Asia/East Asia (Fig. 6; Table S9). The crown age of *Lecanopteris* s.s. was dated back to the middle Neogene around 11 Ma (node 96; HPD = 10.54–11.61 Ma) with the subsequent establishment of the other lineage during the late Miocene to the middle Quaternary (node 78 → 94) (Fig. 6; Table S9). The ancestral crown area of *Lecanopteris* s.s. was most likely in Continental Asia/East Asia plus Sundaic region (Fig. 6; Table S9). A total of 12 dispersal events were inferred, which covered nearly all nodes of the genus *Lecanopteris* s.s. (Fig. 6). Besides, five vicariance events have been detected in the node 80, node 85, node 90, node 91, and node 96 (Fig. 6).

3.6.2. Nuclear biogeography

Molecular dating result suggested that the split between Platycerioideae and Microsoroideae was around the middle Eocene (node 64;

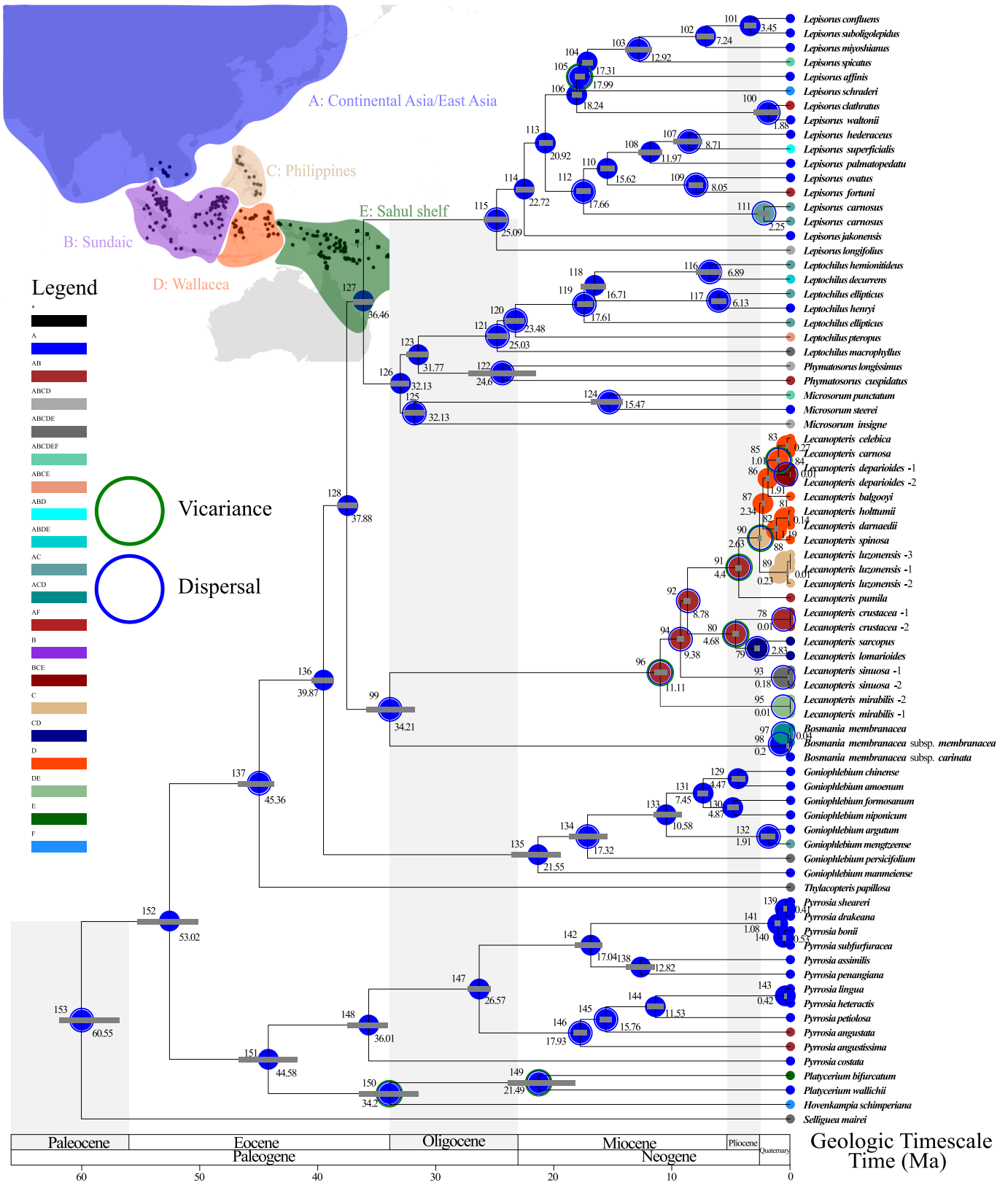

Fig. 6. Time-calibrated phylogeny of *Lecanopteris* s.s.. The times were inferred by treePL based on PT_R dataset. The divergence times are shown above the nodes, and the number of the node are shown behind the nodes. Ancestral range estimation used BioGeoBEARS to implement in RASP under the BAYAREALIKE+J model. The single-most-probable state (geographical range) is shown at each node. Grey bars on nodes indicate the 95% highest probability density interval of the age. Maps show the distribution of species based on Global Biodiversity Information Facility (GBIF) data as black points for the genus *Lecanopteris* s.s..

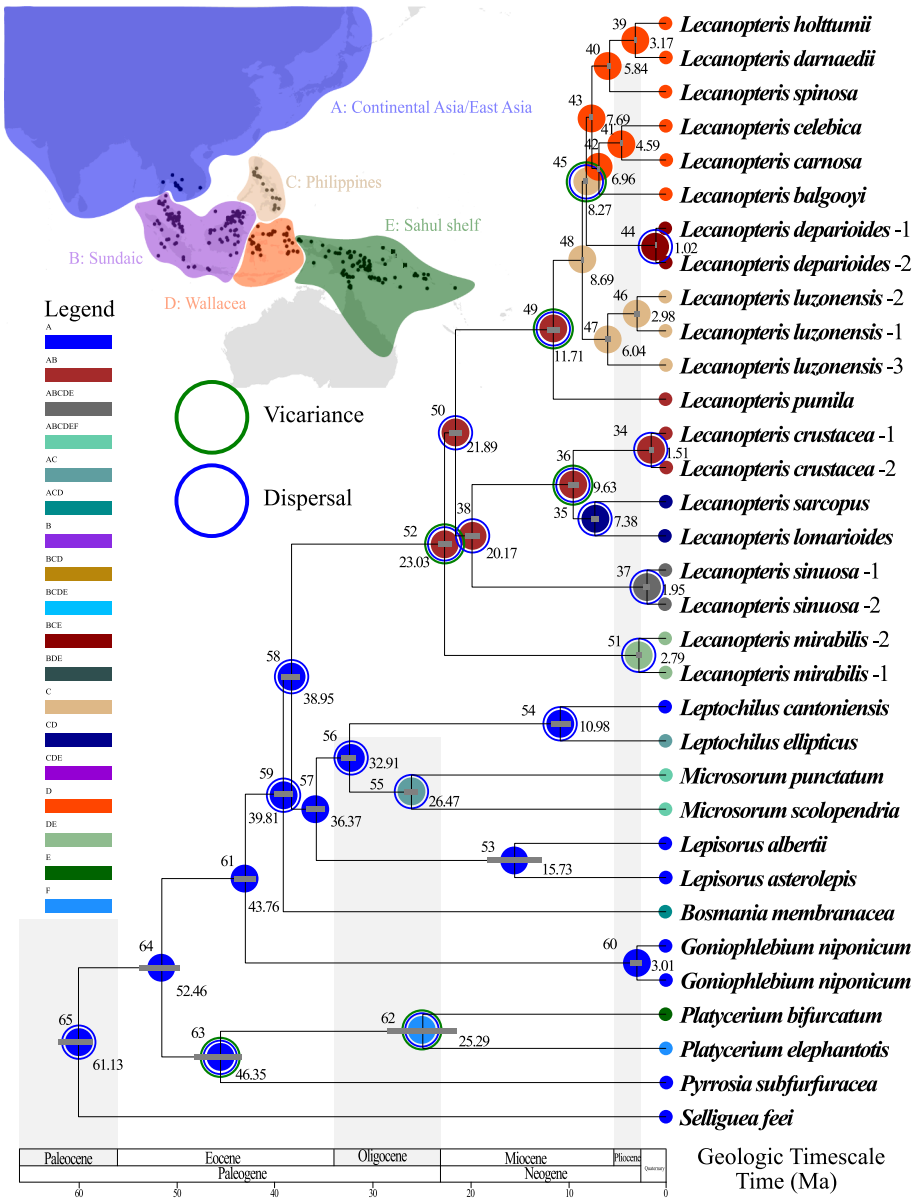

Fig. 7. Time-calibrated phylogeny of *Lecanopteris* s.s.. The times were inferred by treePL based on TT_R dataset. The divergence times are shown above the nodes, and the number of the node are shown behind the nodes. Ancestral range estimation used BioGeoBEARS to implement in RASP under the BAYAREALIKE+J model. The single-most-probable state (geographical range) is shown at each node. Grey bars on nodes indicate the 95% highest probability density interval of the age. Maps show the distribution of species based on Global Biodiversity Information Facility (GBIF) data as black points for the genus *Lecanopteris* s.s..

HPD = 50.61–54.84 Ma) (Fig. 7; Table S10). Although the limited outgroup samples were included, the reconstructed distribution ranges for Microsoroideae were also inferred in Continental Asia/East Asia (Fig. 7; Table S10). The crown age of the genus *Lecanopteris* s.s. was dated to the Oligocene–Miocene boundary around 23.03 Ma (node 52; HPD = 22.33–23.70 Ma) (Fig. 7; Table S10). Continental Asia/East Asia and Sundaic region were also proposed as the most likely ancestral distribution regions of *Lecanopteris* s.s. (Fig. 7; Table S10). The almost lineages of *Lecanopteris* s.s. were established during the Neogene (Fig. 7; Table S10). A total of 11 dispersal events and three vicariance events were inferred (Fig. 7).

4. Discussion

4.1. Unique genomic structure

The plastome of ferns generally ranges from 130 kb to 170 kb in length (Grewe et al., 2013; Zhong et al., 2014; Lu et al., 2015). In this study, the plastome sizes varied considerably within a single genus of *Lecanopteris* s.s. (Table 3; Fig. 1). Except for the plastome sizes of the crustacea group (151–167 kb) were same as most of the ferns, the pumila group and the darnaedii group have the largest plastome size (178–187 kb). More than 600 fern plastomes have been sequenced and we found that the *Lecanopteris* s.s. has the largest plastome size except for *Asplenium yoshinagae* Makino (186 kb; OM419356; Aspleniaceae). Three species of *Selliguea* (172–178 kb; MT130547, MT130580, MT130663, MW876368, OM419351; Drynarioideae), two species of *Saccoloma* (171–174 kb; MT130580, MT130691, NC044686; Saccolomataceae), and one species of *Matonia* (172 kb; OM419375; Matoniaceae) also have large plastome genome size (Lehtonen and Cárdenas, 2019; Wei et al., 2021; Du et al., 2021; Du et al., 2022). Previous studies have found that several factors contribute to the wide variation in genome size (Jansen and Ruhlman, 2012; Mower and Vickrey, 2018): (1) expansion/contraction and loss of the IR; (2) gene loss and additional

gene duplications outside of the IR; (3) variation in the size of introns and intergenic spacer regions. We identified the large plastomes size of *Lecanopteris* s.s due to extreme IR expansion toward the SSC region. Like the plastome of *Asplenium yoshinagae* and five samples of *Selliguea* in which the SSC contain no gene (or less than 50 bp in size; Du et al., 2022), also do not contain any genes and SSC sizes only had 119 bp to 234 bp (Table 3; Fig. 1). At the structural level, the *Lecanopteris* s.s plastomes are largely collinear, and the IR expansions can explain the structural rearrangements among different lineages (Fig. 1).

Across ferns, each plastome tends to contain approximately 80 protein-coding genes, 4 rRNAs, and 30 tRNAs (Kuo et al., 2018; Du et al., 2022). *Lecanopteris* s.s plastid gene content seems to vary widely among different lineages (Table 3; Fig. 1). Compared with the crustacea group and the pumila group + the darnaedii group, 17 genes (*ccs*A, *chl*L, *chl*N, *ndh*A, *ndh*D, *ndh*E, *ndh*F, *ndh*G, *ndh*H, *ndh*I, *psa*C, *rpl*21, *rpl*32, *rps*15, *trn*L, *trn*P, *ycf*1) had two copies due to the IR expansions (Fig. 1). Plastome gene content reduction is generally speculated to be the result of a low-cost strategy that could facilitate rapid genome replication under disadvantageous environmental conditions (McCoy et al., 2008; Wu et al., 2009; Martín and Sabater, 2010). Potentially, the copy of the 17 plastid genes could be correlated with the high-altitude habitat of *Lecanopteris* s.s. All species of the crustacea group mainly inhabit the lowland rain forest except for *L. mirabilis*, which mainly inhabits the mid-montane rainforest (Gay et al., 1994). By contrast, all species of the pumila group and the darnaedii group mainly inhabit the mid-montane rainforest and summit or ridgetop vegetation, except for *L. luzonensis*, which mainly inhabits in the lowland rain forest (Gay et al., 1994). It's worth mentioning that all species of *Lecanopteris* s.s always contain 104 protein-coding genes, 33 tRNA genes, and eight rRNA genes (Fig. 1), which implied that these genes can ensure the central functions of the chloroplast, such as photosynthesis and carbon fixation.

4.2. *Lecanopteris s.s. Phylogenomics*

Due to the highly diverse morphological traits, the circumscription of lecanopteroid ferns has greatly changed since Gay et al. (1994) published the first monograph of this genus (Ching, 1940; Jermy and Walker, 1975; Gay et al., 1994; Hennipman and Hovenkamp, 1998; Haufler et al., 2003; Kreier et al., 2008; PPG I 2016; Testo et al., 2019; Chen et al., 2020, 2021; Perrie et al., 2021; Wei and Zhang, 2022). In this study, our plastome-based results are largely consistent with previous studies based on limited plastid markers (Haufler et al., 2003; Kreier et al., 2008; Testo et al., 2019), albeit with stronger support (Fig. 2, Fig. S1). Either plastome-based or nuclear-based, the inferred phylogenetic had demonstrated that the pumila group and the crustacea group were paraphyletic (Fig. 2 and 3, Figs. S1 and S2).

The crustacea group always divided into three major lineages and as the first diverged lineages of *Lecanopteris* s.s. (Figs. 2 and 3, Figs. S1 and S2). We also supported Jermy and Walker (1975) statement that the crustacea group (=subgenus *Myrmecopteris*) was ancestral in the genus of *Lecanopteris* s.s., which have a less specialized pattern of growth and development compared to other *Lecanopteris* s.s. species. Gay (1993a) had stated two hypotheses for the origin of the subgenus *Myrmecopteris*: (1) *L. mirabilis* and/or *L. sarcopus* (=*L. lomarioides*); (2) *L. sinuosa*. The well-supported evolutionary history of *Lecanopteris* s.s. is here supported that *L. mirabilis* can be regarded as sister to the other *Lecanopteris* s.s. species (Figs. 2 and 3, Figs. S1 and S2). *L. crustacea* is sister to *L. mirabilis* and *L. sarcopus* which is also supported by morphological characters such as raphyses, a common sporangium shape, and 16 spores per sporangium. Other possible relationships within *Lecanopteris* s.s. have been proposed. For instance, *L. spinosa*, proposed by Jermy and Walker (1975) as "intermediate" between the subgenus *Myrmecopteris* (= the crustacea group) and the subgenus *Lecanopteris* (= the pumila group + the darnaedii group), but Hennipman (1986) thought it might be a member of the subgenus *Lecanopteris* (= the pumila group + the darnaedii group. Actually, *L. spinosa*, as currently construed, should be a member of the subgenus *Myrmecopteris* (= the crustacea group) (Figs. 2 and 3, Figs. S1 and S2). The monophyly of the darnaedii group has been confirmed here with high support (Figs. 2 and 3, Figs. S1 and S2), all three members of this group have a two-gallery system (Gay, 1993a; Gay et al., 1994). In previous morphological studies, *Lecanopteris deparioides* has been considered basal to the other members of Subgenus. *Lecanopteris* for which has the widest geographic range and a simple rhizome architecture, and the species of the pumila group might have arisen from the darnaedii group (Gay, 1993a, b; Gay et al., 1994; Hennipman, 1989). Without consideration of the two hybrids in cultivation, our results and previous phylogenetic results both revealed that *L. pumila* is the sister species among all the other species of the subgenus. *Lecanopteris* (Figs. 2 and 3, Figs. S1 and S2; Haufler et al., 2003; Kreier et al., 2008; Testo et al., 2019). Although the relationship of the ants and the evolution of *Lecanopteris* s.s. be a challenging task (Gay, 1993a), the morphology and architecture of the rhizome of *Lecanopteris* s.s. were not much homoplasious, which unequally distributed in three groups and thus useful to characterize the genus morphologically based on the previous studies (Gay, 1993a, b; Gay et al., 1994; Hennipman, 1989) and our observations. Beginning with the crustacea group, *L. mirabilis* has a solid, arched rhizome, with the domatium between the rhizome underside and host trunk; *L. sinuosa* has hollow rhizomes and phyllopodia; *L. sarcopus* and *L. lomarioides* displays dimorphism between solid frond-hearing axes and hollow, frondless side branches; the rhizome of *L. crustacea* is hollow but phyllopodia are solid; *L. sinuosa* has hollow rhizomes and phyllopodia. The pumila group have a central gallery and hollow phyllopodia, but the darnaedii group have two gallery and chamber systems.

4.3. *Cytonuclear discordance as further evidence for gene flow*

Phylogenetic analyses based on the nuclear and plastome datasets resulted in conflicts (Figs. 2-4, Figs. S1 and S2). The conflicting signals were detected within both plastid and nuclear genes through Phyparts and QS analyses (Fig. 4). Additionally, conflicting degrees detected by two datasets (PT and TT) were inconsistent (Fig. 4). Both Phyparts and QS analyses revealed few conflicts within the PT dataset (Fig. 4a). In contrast, the conflict analyses of Phyparts and QS analyses exhibited a higher degree of discordance with the concatenated phylogenetic tree (Fig. 4b). Many factors could cause incongruent tree topologies among nuclear genes or between nuclear and plastome genes, such as ILS, hybridization, hidden paralogs, recombination, chloroplast capture, and horizontal gene transfer (Degnan and Rosenberg, 2009; Walker et al., 2018; Wang et al., 2018; Morales-Briones et al., 2021). The estimated theta parameter, which could reflect the level of ILS (Cai et al., 2020). Almost all ancestor branches of the species of *Lecanopteris* s.s. showed a relatively lower level of ILS, except the ancestor branches of the pumila group and the darnaedii group showed the highest level of ILS based on TT dataset (Fig. 5a). The simulated gene trees based on TT datset under ILS condition also showed a relative agreement with the empirical trees (R^2 = 0.66 or 0.92) (Fig. 5c-d), but showed a highly agreement with empirical trees (R^2 = 0.94 or 0.99) based on TT_R dataset which was removed the two cultivated hybrids (*L.* 'Yellow Tip', and *L.* 'Tatsuta') (Fig. S3c-d). This suggests that ILS alone cannot explain the high level of cytonuclear discordance observed in *Lecanopteris* s.s..

In addition to ILS, gene flow can also explain gene tree conflict and/or cytonuclear discordance. The QuIBL analysis based on different datasets revealed that 50.8% or 52.5% of the tested triplets showed significant evidence for introgression (2,346 out of 4,620 triplets or 1,794 out of 3,420 triplets, $\Delta BIC > 10$) (Tables S4 and S5; Fig. 5e, Fig. S3e), suggesting phylogenetic uncertainties caused by gene flow between lineages rather than ILS (Meleshko et al., 2021; Qian et al., 2023). In addition, the phylogenetic positions of the conflict were mainly located among the pumila group + the darnaedii group lineage (Figs. 2-4, Figs. S1 and S2). We found evidence of extensive introgression in these lineages when we divided all the QuIBL results into species pairs and calculated the average of the total introgression proportion for each

species pair (Tables S4 and S5; Fig. 5b, Figs. 2 and 3, Fig. S3b). The QuIBL result implied that introgression plays a more substantial role than ILS in underpinning phylogenetic discordance in *Lecanopteris* s.s., especially in the pumila group and the darnaedii group lineages (Tables S4 and S5; Fig. 5b, Fig. S3b) (Edelman et al., 2019). The HyDe results also support past gene flow occurring frequently within *Lecanopteris* s.s. (503 out of 694 hypotheses or 371 out of 475 hypotheses of hybridization events; Tables S6 and S7) (Hodel et al., 2021; Liu et al., 2022; Nie et al., 2023). Only a small number of hybridization events can be inferred in PhyloNet analysis because PhyloNet can only accommodate limited taxon sampling and computational restrictions (Yu and Nakhleh, 2015). Species with alternative phylogenetic positions are generally depicted as hybrids in the network analyses (Fig. 5g-k). Apart from the two hybrids (*L.* 'Yellow Tip', *L.* 'Tatsuta') in cultivation, both HyDe and PhyloNet analyses also demonstrated that there were amount of hybridization events inferred in other members of *Lecanopteris* s.s. (Tables S6 and S7; Fig. 5i-k, Fig. S3g-k). Therefore, we suggested that gene flow might have resulted in the phylogenetic discordance of *Lecanopteris* s.s.. Furthermore, the reticulate speciation likely also explains the low concordance of gene trees, as suggested by Phyparts and QS analyses.

4.4. The hybrid origin of Lecanopteris 'Yellow Tip' and L. 'Tatsuta'

Lecanopteris s.s. has attracted a number of people who are passionate about ant associated plants. However, no hybrids have ever been reported to occur in the wild (Gay, 1993a, b; Gay et al., 1994), but a few hybrids are known to have arisen in cultivation. *L.* 'Alford', *L.* 'Yellow Tip', and *L.* 'Tatsuta' are the most famous cultivars in *Lecanopteris* s.s. How did these horticultural varieties come about? *L.* 'Alford' was thought to be a hybrid between *L. deparioides* and *L. mirabilis*. *L.* 'Yellow Tip' is characterized by large hollow rhizomes that are bright green, with yellow spines (new growth) when young before eventually changing into a dark brown colour. *L.* 'Tatsuta', a hybrid developed by Carlos Tatsuta, forms rounded, hollow green spotted rhizomes, whose growing points are in deep pink. The rich green fronds ca. 10 inches above the clump. Both are considered cultivated hybrid species. However, their parental sources have always been unclear. Because plastids are likely maternally inherited in ferns (Bell et al., 1966; Sears, 1980; Gastony and Yatskievych, 1992; Vogel et al., 1998), it is possible to detect introgression and/or hybrid speciation by studying cytonuclear discordance (Linder and Rieseberg, 2004). biparentally inherited nuclear genes can also provide important references for the speciation of hybrids (Landrein et al., 2017; Guo et al., 2023; Hu et al., 2023).

Lecanopteris 'Yellow Tip' was previously considered a hybrid between *L. pumila* and *L. luzonensis*. We have integrated multiple sources of evidence to confirm this hypothesis for the first time. A total of 20 out of the 694 hypotheses tested by HyDe showed significant evidence of the hybrid origin of *L.* 'Yellow Tip' (Table S6). In the analyses of plastid data, *L.* 'Yellow Tip' was found to be successively sister to *L. luzonensis* (Figs. 2, 4a) and the plastomes of *L.* 'Yellow Tip' and *L. luzonensis* −2 are 99.9 % identical identity and differ in 188 sites. The nuclear-based phylogenetic analyses recovered maximum support (ML-BS=100, MP-JK=100, BI-PP=1.0, AS-LPP=1.0) for relationships within *L.* 'Yellow Tip' and *L. pumila* (Figs. 3, 4b). The robust phylogeny presented here implies that *L. luzonensis* was the maternal parent of *L.* 'Yellow Tip', while *L. pumila* might be the most possible paternal parent of *L.* 'Yellow Tip' (Figs. 2, 3, 4). Furthermore, *L.* 'Yellow Tip' had an inheritance probability of 0.548–0.565 from the *L. pumila* lineage and 0.435–0.452 from the *L. luzonensis* lineage in each of the four reticulation events (Fig. 5h-k). Based on the results of flow cytometry (Table 4), *L. pumila*, *L. luzonensis*, and *L.* 'Yellow Tip' were all diploid, while *L.* 'Yellow Tip' was heterodiploid. The previously assumption is that *L.* 'Tatsuta' has more parental origins: (1) *L. crustacea* (2x) × *L. mirabilis* (8x); (2) *L. celebica* (2x) × *L. deparioides* (2x). HyDe showed 78 significant hybridization events, which is one of the pieces of evidence for the hybrid origin of *L.* 'Tatsuta' (Table 4, Table S6). The topology of the plastid phylogenetic trees confirmed the sister relationship between *L.* 'Tatsuta' and *L. luzonensis* (Figs. 2, 4a) and the plastomes of *L.* 'Tatsuta' and *L. luzonensis* −2 are nearly 100 % identical identity and differ in 45 sites. In network analyses, *L.* 'Tatsuta' (2x) was reported as a hybrid which gene flow from *L. luzonensis* (2x) and the ancestors of *L. crustacea* (2x) being detected in all five examinations (Table 4; Fig. 5g-k), with an inheritance probability of 0.522 to 0.532 from ancestors of *L. crustacea* and an inheritance probability of 0.478 to 0.488 from *L. luzonensis*. *L.* 'Tatsuta' actually is a hybrid between *L. luzonensis* and *L. crustacea*.

4.5. Biogeographic history of Lecanopteris s.s

The time-calibrated phylogeny reveals that the common ancestor of *Lecanopteris* s.s. diverged in the early Neogene around 23 Ma (HPD = 22.33–23.79 Ma) based on nuclear sequence data (Fig. 7; Table S10). Plastome data produced a relatively younger age for the divergence of the genus in the middle Neogene around 11 Ma (HPD = 10.54–11.61 Ma) (Fig. 6; Table S9). The plastome based divergence time is consistent with Chen et al. (2022), who also suggested the divergence of the crown age of *Lecanopteris* at ca. 11 Ma based on four plastid makers. The different results (plastome-based vs. nuclear-based) could be explained by two hypotheses. The first would suggest the different taxa sampling (Schuettpelz and Pryer, 2009; Testo and Sundue, 2016; Qi et al., 2018; Shen et al., 2018; Du et al., 2021; Pelosi et al., 2022). The second may have simply resulted from different evolutionary rates between these two genomic sequences (Drouin et al., 2008). The estimation of ancestral ranges under the best-fit model (BAYAREALIKE+J) always suggests that the ancestral range of the crown group of *Lecanopteris* s.s. was in the regions of today's Continental Asia/East Asia (A), and Sundaic (B) (Figs. 6, 7; Tables S9 and S10).

The extant species of the pumila group and the darnaedii group show preferences for cool habitats in the mid to high altitudes of Southern East Asia (Gay et al., 1994). Our results could be explained by the hypothesis that members of the *Lecanopteris* s.s. like some lineages of land plants are well adapted to relatively cool environments, and an increase in the Earth's temperature in the late Palaeocene and early Eocene may have forced them to move to higher elevations (Friis, 1985; Manchester, 2000; Wang et al., 2021; Nie et al., 2023). Starting from the cold phase of the Early Oligocene (Zachos et al., 2001). Due to the decreased CO_2 concentration, the high-latitude *Lecanopteris* s.s. from Continental Asia/East Asia dispersed to low latitude (Figs. 6, 7; Tables S9 and S10). Divergence time estimation shows that most lineages of *Lecanopteris* s.s. diversified during the Middle Miocene Climatic Optimum (MMCO) (Figs. 6, 7; Tables S9 and S10), which is consistent with the results of previous studies (Schuettpelz and Pryer, 2009; Testo and Sundue, 2016; Chen et al., 2022). During MMCO, the elevated temperatures likely led to a swift growth of rainforests and a sudden rise in the number of canopy niches, alongside an overall increase in atmospheric humidity, all of which are conducive to the proliferation of epiphytes, and the cold-adapted survivors of warmer climates may have flourished and shifted into new geographic areas (Watkins and Cardelús, 2012; Benton et al., 2021). Schneider et al. (2010) also have proposed that the warming climate during the late Oligocene period could have facilitated the expansion of tropical plant ranges and potentially led to the emergence of swift adaptive radiations. According to the mean ages of splits from a

most recent common ancestor, at least three species evolved in *Lecanopteris* s.s. during the Pleistocene, indicating that sea-level changes could have resulted in substantial speciation (Figs. 6, 7; Tables S9 and S10). Sea levels were much lower during glacial periods and during inter-glacial periods land areas would have contracted into islands 'refugia', which may have resulted in allopatric speciation (Voris, 2000). Although it is, of course, possible that other reasons might have caused speciation. The current allopatric distribution is probably the result of transoceanic dispersal. Dispersal seems to have played an important role in the biogeographic history of *Lecanopteris* s.s., with at least 13 dispersal events inferred based on different datasets, but six vicariance events (Figs. 6, 7). The dispersal might be via spores which had been proved in varies ferns lineages (e.g., Sundue et al., 2014; Wei et al., 2015; Kuo et al., 2016). Fern spores are minute and may have been transported across oceans by the prevailing monsoon wind systems or using ocean currents between islands (Smith, 1993; Kessler, 2010). Besides, hybridization inference had detected some amount of ancient hybridization events (Tables S6, S7) and significant levels of introgression (Tables S4, S5; Fig. 5e, Tables S3e) also implied that a higher probability of gene flow occurred though dispersal during the glacial periods. In addition to climate, geographical changes such as widespread orogenic events and continental uplift during the Miocene also changed the topography, which created various new habitats to host novel plant diversity (Potter and Szatmari, 2009). For example, the collision between India and Asia (~35 Ma or ~ 22–25 Ma) altered the formation of landforms and climate zones in the region of Indochina (Aitchison et al., 2007; Ali and Aitchison, 2008; Van Hinsbergen et al., 2012), and the collision of the Eurasian and Australian plates at the Eocene–Oligocene boundary onwards resulted in the creation of additional Islands (Hall, 2009). In generally, the phylogenomic and biogeographic results are in accordance with the paleoclimate evidence, which suggest that the genus appeared and then establishment of other lineages (Figs. 6, 7; Tables S9 and S10).

5. Future perspectives

Lecanopteris s.s. is one of the most well-known myrmecophytic fern, attracting many plant enthusiasts. With the most comprehensive sampling to date, our phylogenomic analyses have resolved the relationships between species in this genus, and provided a foundation for future taxonomic and phylogenomic studies in Microsoroideae. The phylogenomic results herein found that *L. luzonensis* was divided into two or three groups (Figs. 2 and 3, Fig. S1 and S2). Besides, the gene flow had found that *L. luzonensis* −3 had gene flow from the *L. luzonensis* lineage and the *L. darnaedii* + *L. holttumii* lineage (Fig. 6i-k, S3g-k). Together, these results suggest the need to study on the cryptic taxa within *L. luzonensis*.

The robust phylogeny presented here will allow for improved biogeographical, ecological, and evolutionary interpretations of the Microsoroideae is widely distributed in the tropical and subtropical regions of the Old World and Oceania (Kreier et al., 2008; PPG I, 2016; Chen et al., 2020). The potential limitation of this study was the limited samples of outgroup (see Materials and Methods). Due to absence from our sampling of the closest sisters *Dendroconche* and *Zealandia* (Figs. 2 and 3, Figs. S1 and S2), the monophyletic and biogeography of *Lecanopteris* s.l. need further study. Additionally, while our data suggest the presence of two distinct cytotypes, further studies involving more detailed ploidy analyses (e.g., chromosome count, karyotype analysis) would be necessary to conclusively determine the exact ploidy levels within each cytotype. At genus level, previous studies provide an infrageneric classification largely based on a few chloroplast genes and/or morphological evidence, resulting in conflicting concepts of the classification of these ferns. Various authors have proposed several related genera within the microsoroid ferns (Ching, 1940, 1978; Hennipman and Roos, 1983; Hetterscheid and Hennipman, 1984; Bosman, 1991; Hennipman, 1990; Van Uffelen, 1992, 1993, 1997; Nooteboom, 1997; Smith et al., 2006; Wang et al., 2010a, b; PPG I, 2016; Testo et al., 2019; Chen et al., 2020, 2021; Zhang et al., 2020; Zhao et al., 2020; Perrie et al., 2021; Wei et al., 2021; Wei and Zhang, 2022). Given the morphological similarity, disparity does not accurately reflect the delimitation and the potential reticulate relationship, taking *Lepisorus* (J. Sm.) Ching as an example, we advocate integrating nuclear gene data, estimating molecular time, and considering other evidence which will be helpful to establish a robust infrageneric classification.

CRediT authorship contribution statement

Li-Ju Jiang: Conceptualization, Investigation, Resources, Writing – original draft, Writing – review & editing, Visualization, Supervision. **Jing Zhao:** Conceptualization, Resources, Writing – original draft, Writing – review & editing, Visualization. **Jia-Guan Wang:** Investigation, Resources. **Sven Landrein:** Investigation. **Ji-Pu Shi:** Investigation. **Chuan-Jie Huang:** Investigation. **Miao Luo:** Investigation. **Xin-Mao Zhou:** Investigation. **Hong-Bin Niu:** Investigation, Resources, Writing – review & editing, Supervision. **Zhao-Rong He:** Writing – review & editing, Supervision, Funding acquisition, Writing – review & editing, Supervision.

Declaration of competing interest

The authors declare that they have no known competing financial interests or personal relationships that could have appeared to influence the work reported in this paper.

Data availability

Multiple sequence alignments, concatenated alignments, and phylogenetic trees are available at Figshare: https://doi.org/10.6084/m9.figshare.25309648.v1

Acknowledgements

The authors thank the support of Yunnan Provincial Department of Education Science Research Fund Project (Grant No. 2023Y0202), Conservation of Wild Plants with Extremely Small Populations -Advancing Artificial Propagation Techniques and Constructing Ex-Situ living collections of Four Tropical Plant Species with Extremely Small Populations (Grant No. 2023SJ09X-07), Flora of Pan-Himalaya (Grant No. 31620103902), Yunnan Fundamental Research Projects (Grant No. 202301BF07001-016), and National Science & Technology Fundamental Resources Investigation Program of China (Grant No. 2022FY100201). We are very grateful to Xiong Li for help on flow cytometry, Zhang-Ming Zhu, Lei Wang, and Ting Wang for their help on data analysis. The authors also thank the two anonymous reviewers and editors for their critiques and suggestions which greatly improved our manuscript.

Appendix A. Supplementary data

Supplementary data to this article can be found online at https://doi.org/10.1016/j.ympev.2024.108199.

References

Aitchison, J.C., Ali, J.R., Davis, A.M., 2007. When and where did India and asia collide? J. Geophys. Res. 112, B05423. https://doi.org/10.1029/2006JB004706.

Ali, J.R., Aitchison, J.C., 2008. Gondwana to Asia: Plate tectonics, paleogeography and the biological connectivity of the Indian subcontinent from the Middle Jurassic through latest Eocene (166–35 Ma). Earth-Sci. Rev. 88, 145–166. https://doi.org/10.1016/j.earscirev.2008.01.007.

Almeida, T.E., 2018. Ant-fern association in *Microgramma megalophylla*. Am. Fern J. 108, 62–64. https://doi.org/10.1640/0002-8444-108.2.62.

Bell, P., Frey-Wyssling, A., Mühlethaler, K., 1966. Evidence for the discontinuity of plastids in the sexual reproduction of a plant. J. Ultrastruct. Res. 15, 108–121. https://doi.org/10.1016/s0022-5320(66)80098-9.
Benton, M.J., Wilf, P., Sauquet, H., 2021. The Angiosperm terrestrial revolution and the origins of modern biodiversity. New Phytol. 233, 2017–2035. https://doi.org/10.1111/nph.17822.
Blischak, P.D., Chifman, J., Wolfe, A.D., Kubatko, L.S., 2018. HyDe: A python package for genome-scale hybridization detection. Syst. Biol. 67, 821–829. https://doi.org/10.1093/sysbio/syy023.
Bosman, M.T.M., 1991. A monograph of the fern genus *Microsorum* (Polypodiaceae), including an attempt towards a reconstruction of the phylogenetic history of the microsoroids. Leiden Bot. Ser. 14, 1–161.
Buerki, S., Forest, F., Alvarez, N., Nylander, J.A.A., Arrigo, N., Sanmartın, I., 2011. An evaluation of new parsimony-based versus parametric inference methods in biogeography: a case study using the globally distributed plant family Sapindaceae. J. Biogeogr. 38, 531–550. https://doi.org/10.1111/j.1365-2699.2010.02432.x.
Buerki, S., Forest, F., Alvarez, N., 2014. Proto-South-East Asia as a trigger of early angiosperm diversification. Bot. J. Linn. Soc. 174, 326–333. https://doi.org/10.1111/boj.12129.
Cai, S., Cai, X., Li, S., Liu, S., Wang, Z., Wang, T., Su, Y., 2018. The complete chloroplast genome of *Pyrrosia bonii* (Polypodiaceae), an important ornamental and medical fern. Mitochondrial DNA B Resour. 3, 801–802. https://doi.org/10.1080/23802359.2018.1491347.
Cai, L.-M., Xi, Z.-X., Lemmon, E.M., Lemmon, A.R., Mast, A., Buddenhagen, C.E., Liu, L., Davis, C.C., 2020. The perfect storm: Gene tree estimation error, incomplete lineage sorting, and ancient gene flow explain the most recalcitrant ancient angiosperm clade. Malpighiales. Syst. Biol. 70, 491–507. https://doi.org/10.1093/sysbio/syaa083.
Campbell, L.C.E., Kiers, E.T., Chomicki, G., 2023. The evolution of plant cultivation by ants. Trends Plant Sci. 28, 271–282. https://doi.org/10.1016/j.tplants.2022.09.005.
Capella-Gutierrez, S., Silla-Martinez, J.M., Gabaldon, T., 2009. trimAl: A tool for automated alignment trimming in large-scale phylogenetic analyses. Bioinformatics 25, 1972–1973. https://doi.org/10.1093/bioinformatics/btp348.
Chan, P.-P., Lowe, T.M., 2019. tRNAscan-SE: Searching for tRNA genes in genomic sequences. Methods Mol. Biol. 1962, 1–14. https://doi.org/10.1007/978-1-4939-9173-0_1.
Chen, C.-C., Hyvönen, J., Schneider, H., 2020. Exploring phylogeny of the microsoroid ferns (Polypodiaceae) based on six plastid DNA markers. Mole. Phylogenet. Evol. 143, 106665 https://doi.org/10.1016/j.ympev.2019.106665.
Chen, C.-C., Liu, H.-Y., Chen, C.-W., Schneider, H., Hyvönen, J., 2021. On the spore ornamentation of the microsoroid ferns (Microsoroideae, Polypodiaceae). J. Plant Res. 134, 55–76. https://doi.org/10.1007/s10265-020-01238-4.
Chen, C.-C., Hyvönen, J., Schneider, H., 2022. Re-terrestrialization in the phylogeny of epiphytic plant lineages: Microsoroid ferns as a case study. J. Syst. Evol. 61, 613–626. https://doi.org/10.1111/jse.12899.
Chen, S., Zhou, Y., Chen, Y., Gu, J., 2018. Fastp: An ultra-fast all-in-one FASTQ preprocessor. Bioinformatics 34, i884–i890. https://doi.org/10.1093/bioinformatics/bty560.
Ching, R.-C., 1940. On natural classification of the family "Polypodiaceae". Sunyatsenia 5, 201–268.
Ching, R.-C., 1978. The Chinese fern families and genera: Systematic arrangement and historical origin. Acta Phytotax. Sin. 16, 16–37.
Cox, C.B., Moore, P.D., Ladle, R.J., 2016. Biogeography: A ecological and evolutionary approach, Ninth Edition. Wiley Blackwell, Oxford.
Danecek, P., Bonfield, J.K., Liddle, J., Marshall, J., Ohan, V., Pollard, M.O., Whitwham, A., Keane, T., McCarthy, S.A., Davies, R.M., Li, H., 2021. Twelve years of SAMtools and BCFtools. GigaScience 10, giab008. https://doi.org/10.1093/gigascience/giab008.
Davidson, D.W., McKey, D., 1993. The evolutionary ecology of symbiotic ant–plant relationships. J. Hym. Res. 2, 13–83. https://doi.org/10.5962/BHL.PART.29733.
Degnan, J.H., Rosenberg, N.A., 2009. Gene tree discordance, phylogenetic inference and the multispecies coalescent. Trends Ecol. Evol. 24, 332–340. https://doi.org/10.1016/j.tree.2009.01.009.
Doyle, J.J., 1987. A rapid DNA isolation procedure for small amounts of fresh leaf tissue. Phytochem. Bull. 19, 11–15. https://doi.org/10.1016/0031-9422(80)85004-7.
Drouin, G., Daoud, H., Xia, J., 2008. Relative rates of synonymous substitutions in the mitochondrial, chloroplast and nuclear genomes of seed plants. Mol. Phylogenet. Evol. 49, 827–831. https://doi.org/10.1016/j.ympev.2008.09.009.
Drummond, A.J., Suchard, M.A., Xie, D., Rambaut, A., 2012. Bayesian phylogenetics with BEAUti and the BEAST 1.7. Mol. Biol. Evol. 29, 1969–1973. https://doi.org/10.1093/molbev/mss075.
Du, X.-Y., Lu, J.-M., Lu, S.-G., Li, D.-Z., 2019. Complete plastome of an endemic fern species from China: *Neocheiropteris palmatopedata* (Polypodiaceae). Mitochondrial DNA B Resour. 4, 2394–2395. https://doi.org/10.1080/23802359.2018.1532840.
Du, X.-Y., Lu, J.-M., Zhang, L.-B., Wen, J., Kuo, L.-Y., Mynsseng, C.M., Schneider, H., Li, D.-Z., 2021. Simultaneous diversification of Polypodiales and angiosperms in the Mesozoic. Cladistics 37, 518–539. https://doi.org/10.1111/cla.12457.
Du, X.-Y., Kuo, L.-Y., Zuo, Z.-Y., Li, D.-Z., Lu, J.-M., 2022. Structural variation of plastomes provides key insight into the deep phylogeny of ferns. Front. Plant Sci. 13, 862772 https://doi.org/10.3389/fpls.2022.862772.
Edelman, N.B., Frandsen, P.B., Miyagi, M., Clavijo, B., Davey, J., Dikow, R.B., García-Accinelli, G., Van Belleghem, S.M., Patterson, N., Neafsey, D.E., Challis, R., Kumar, S., Moreira, G.R.P., Salazar, C., Chouteau, M., Counterman, B.A., Papa, R., Blaxter, M., Reed, R.D., Dasmahapatra, K.K., Kronforst, M., Joron, M., Jiggins, C.D., McMillan, W.O., Di Palma, F., Blumberg, A.J., Wakeley, J., Jaffe, D., Mallet, J., 2019. Genomic architecture and introgression shape a butterfly radiation. Science 366, 594–599. https://doi.org/10.1126/science.aaw2090.
Emms, D.M., Kelly, S., 2019. OrthoFinder: Phylogenetic orthology inference for comparative genomics. Genome Biol. 20, 1–14. https://doi.org/10.1186/s13059-019-1832-y.
Fay, M.F., Forest, F., 2013. Biogeography – different geographical and taxonomic scales. Bot. J. Linn. Soc. 171, 301–303. https://doi.org/10.1111/boj.12019.
Friis, E.M., 1985. Angiosperm fruits and seeds from the Middle Miocene of Jutland (Denmark). Biologiske Skrifter 24, 1–165.
Gastony, G.J., Yatskievych, G., 1992. Maternal inheritance of the chloroplast and mitochondrial genomes in cheilanthoid ferns. Am. J. Bot. 79, 716–722. https://doi.org/10.2307/2444887.
Gay, H., 1993a. Rhizome structure and evolution in the ant-associated epiphytic fern *Lecanopteris* Reinw. (Polypodiaceae). Bot. J. Linn. Soc. 113, 135. https://doi.org/10.1006/bojl.1993.1068.
Gay, H., 1993b. Animal-fed plants: an investigation into the uptake of ant-derived nutrients by the far eastern epiphytic fern *Lecanopteris* Reinw. (Polypodiaceae). Biol. J. Linn. Soc. 50, 221–233. https://doi.org/10.1111/j.1095-8312.1993.tb00928.x.
Gay, H., Hennipman, E., Huxley, C.R., Parrott, F.J.E., 1994. The taxonomy, distribution and ecology of the epiphytic Malesian ant-fern *Lecanopteris* Reinw. (Polypodiaceae). Gardens' Bulletin Singapore. 44, 293–335.
Gonçalves, D.J.P., Simpson, B.B., Ortiz, E.M., Shimizu, G.H., Jansen, R.K., 2019. Incongruence between gene trees and species trees and phylogenetic signal variation in plastid genes. Mol. Phylogenet. Evol. 138, 219–232. https://doi.org/10.1016/j.ympev.2019.05.022.
Grabherr, M.G., Haas, B.J., Yassour, M., Levin, J.Z., Thompson, D.A., Amit, I., Adiconis, X., Fan, L., Raychowdhury, R., Zeng, Q., Chen, Z., Mauceli, E., Hacohen, N., Gnirke, A., Rhind, N., Palma, F.D., Birren, B.W., Nusbaum, C., Lindblad-Toh, K., Friedman, N., Regev, A., 2011. Trinity: Reconstructing a full-length transcriptome without a genome from RNA-Seq data. Nat. Biotechnol. 29, 644–652. https://doi.org/10.1038/nbt.1883.
Grewe, F., Guo, W.H., Gubbels, E.A., Hansen, A.K., Mower, J.P., 2013. Complete plastid genomes from *Ophioglossum californicum*, *Psilotum nudum*, and *Equisetum hyemale* reveal an ancestral land plant genome structure and resolve the position of Equisetales among monilophytes. BMC Evolution. Biol. 13, 8. https://doi.org/10.1186/1471-2148-13-8.
Guo, C., Luo, Y., Gao, L.-M., Yi, T.-S., Li, H.-T., Yang, J.-B., Li, D.-Z., 2023. Phylogenomics and the flowering plant tree of life. J. Integr. Plant Biol. 65, 299–323. https://doi.org/10.1111/jipb.13415.
Haas, B.J., Papanicolaou, A., Yassour, M., Grabherr, M., Blood, P.D., Bowden, J., Couger, M.B., Eccles, D., Li, B., Lieber, M., Macmanes, M.D., Ott, M., Orvis, J., Pochet, N., Strozzi, F., Weeks, N., Westerman, R., William, T., Dewey, C.N., Henschel, R., LeDuc, R.D., Friedman, N., Regev, A., 2013. De novo transcript sequence reconstruction from RNA-seq using the Trinity platform for reference generation and analysis. Nat. Protoc. 8, 1494–1512. https://doi.org/10.1038/nprot.2013.084.
Hall, R., 2009. Southeast Asia's changing palaeogeography. Blumea 54, 148–161. https://doi.org/10.3767/000651909X475941.
Haufler, C.H., Grammer, W.A., Hennipman, E., Ranker, T.A., Smith, A.R., Schneider, H., 2003. Systematics of the ant-fern genus *Lecanopteris* (Polypodiaceae): Testing phylogenetic hypotheses with DNA sequences. Syst. Bot. 28, 217–228. https://www.jstor.org/stable/3093992.
Hennipman, E., 1986. Notes on the ant-ferns of *Lecanopteris* sensu lato in Sulawesi, Indonesia, with the description of two new species. Kew Bull. 41, 783–789. https://doi.org/10.2307/4102977.
Hennipman, E., 1989. The systematics and phytogeography of the Malesian ant-fern genus *Lecanopteris* (Filicales, Polypodiaceae). Proceedings of ISSP 1988, 39.
Hennipman, E., 1990. The significance of the SEM for character analysis of spores of Polypodiaceae (Filicales). In: Claugher, D. (Ed.), Scanning Electron Microscopy in Taxonomy and Functional Morphology. Clarendon Press, Oxford, pp. 23–44.
Hennipman, E., Hovenkamp, P.H., 1998. *Lecanopteris*. Flora Malesiana. Ser. II 3, 59–72.
Hennipman, E., Roos, M.C., 1983. Phylogenetic systematics of the Polypodiaceae (Filicales). Verh. Naturwiss. Vereins Hamburg 26, 321–342.
Hetterscheid, W.L.A., Hennipman, E., 1984. Venation patterns, soral characteristics, and shape of the fronds of the microsorioid Polypodiaceae. Meded. Bot. Mus. Herb. Rijksuniv. Utrecht 540, 11–47.
Hodel, R.G.J., Zimmer, E., Wen, J., 2021. A phylogenomic approach resolves the backbone of *Prunus* (Rosaceae) and identifies signals of hybridization and allopolyploidy. Mol. Phylogenet. Evol. 160, 107118 https://doi.org/10.1016/j.ympev.2021.107118.
Hu, H., Sun, P.-C., Yang, Y.-Z., Ma, J.-X., Liu, J.-Q., 2023. Genome-scale angiosperm phylogenies based on nuclear, plastome, and mitochondrial datasets. J. Integr. Plant Biol. 65, 1479–1489. https://doi.org/10.1111/jipb.13455.
Huson, D.H., Scornavacca, C., 2012. Dendroscope 3: An interactive tool for rooted phylogenetic trees and networks. Syst. Biol. 61, 1061–1067. https://doi.org/10.1093/sysbio/sys062.
Husson, L., Boucher, F.C., Sarr, A., Sepulchre, P., Cahyarini, S.Y., 2019. Evidence of Sundaland's subsidence requires revisiting its biogeography. J. Biogeogr. 47, 843–853. https://doi.org/10.1111/jbi.13762.
Jansen, R.K., Ruhlman, T.A., 2012. Plastid genomes of seed plants. In: Bock, R., Knoop, V. (Eds.), Genomics of Chloroplasts and Mitochondria. Springer, Dordrecht (The Netherlands), pp. 103–126.
Jermy, A.C., Walker, T.G., 1975. *Lecanopteris spinosa*, a new ant-fern from Indonesia. The British Fern Gazette 11, 165–176.

Jin, J.-J., Yu, W.-B., Yang, J.-B., Song, Y., dePamphilis, C.W., Yi, T.-S., Li, D.-Z., 2020. GetOrganelle: A fast and versatile toolkit for accurate de novo assembly of organelle genomes. Genome Biol. 21, 241. https://doi.org/10.1186/s13059-020-02154-5.

Kalyaanamoorthy, S., Minh, B.Q., Wong, T.K.F., von Haeseler, A., Jermiin, L.S., 2017. ModelFinder: Fast model selection for accurate phylogenetic estimates. Nat. Methods 14, 587–589. https://doi.org/10.1038/nmeth.4285.

Katoh, K., Standley, D.M., 2013. MAFFT multiple sequence alignment software version 7: Improvements in performance and usability. Mol. Biol. Evol. 30, 772–780. https://doi.org/10.1093/molbev/mst010.

Kessler, M., 2010. Biogeography of ferns. In: Mehltreter, K., Walker, L.R., Sharpe, J.M. (Eds.), Fern Ecology. Cambridge University Press, Cambridge, pp. 22–46.

Kooyman, R.M., Morley, R.J., Crayn, D.M., Joyce, E.M., Rossetto, M., Slik, J.W.F., Strijk, J.S., Su, T., Yap, J.Y.S., Wilf, P., 2019. Origins and assembly of Malesian rainforests. Ann. Rev. Eco. Evo. Syst. 50, 119–143. https://doi.org/10.1146/annurev-ecolsys-110218-024737.

Koptur, S., 1992. Extrafloral nectary-mediated interactions between insects and plants. In: Bernays, E. (Ed.), Insect–plant Interactions. CRC, Boca Raton, Fla., pp. 81–129

Kreier, H.P., Schneider, H., 2006. Phylogeny and biogeography of the staghorn fern genus *Platycerium* (Polypodiaceae, Polypodiidae). Am. J. Bot. 93, 217–225. https://doi.org/10.3732/ajb.93.2.217.

Kreier, H.P., Zhang, X.-C., Muth, H., Schneider, H., 2008. The microsoroid ferns: Inferring the relationships of a highly diverse lineage of Paleotropical epiphytic ferns (Polypodiaceae, Polypodiopsida). Mol. Phylogenet. Evol. 48, 1155–1167. https://doi.org/10.1016/j.ympev.2008.05.001.

Kuo, L.-Y., Ebihara, A., Shinohara, W., Rouhan, G., Wood, K.R., Wang, C.-N., Chiou, W.-L., 2016. Historical biogeography of the fern genus *Deparia* (Athyriaceae) and its relation with polyploidy. Mol. Phylogenet. Evol. 104, 123–134. https://doi.org/10.1016/j.ympev.2016.08.004.

Kuo, L.-Y., Qi, X., Ma, H., Li, F.-W., 2018. Order-level fern plastome phylogenomics: New insights from Hymenophyllales. Am. J. Bot. 105, 1545–1555. https://doi.org/10.1002/ajb2.1152.

Landis, M.J., Matzke, N.J., Moore, B.R., Huelsenbeck, J.P., 2013. Bayesian analysis of biogeography when the number of areas is large. Syst. Biol. 62, 789–804. https://doi.org/10.1093/sysbio/syt040.

Landrein, S., Buerki, S., Wang, H.-F., Clarkson, J.J., 2017. Untangling the reticulate history of species complexes and horticultural breeds in *Abelia* (Caprifoliaceae). Ann. Bot. 120, 257–269. https://doi.org/10.1093/aob/mcw279.

Lehtonen, S., Cárdenas, G.G., 2019. Dynamism in plastome structure observed across the phylogenetic tree of ferns. Bot. J. Linn. Soc. 190, 229–241. https://doi.org/10.1093/botlinnean/boz020.

Li, H., 2018. Minimap2: Pairwise alignment for nucleotide sequences. Bioinformatics 34, 3094–3100. https://doi.org/10.1093/bioinformatics/bty191.

Li, W., Godzik, A., 2006. Cd-hit: A fast program for clustering and comparing large sets of protein or nucleotide sequences. Bioinformatics 22, 1658–1659. https://doi.org/10.1093/bioinformatics/btl158.

Linder, C.R., Rieseberg, L.H., 2004. Reconstructing patterns of reticulate evolution in plants. Ame. J. Bot. 91, 1700–1708. https://doi.org/10.3732/ajb.91.10.1700.

Liu, B.-B., Campbell, C.S., Hong, D.-Y., Wen, J., 2020a. Phylogenetic relationships and chloroplast capture in the Amelanchier-Malacomeles-Peraphyllum clade (Maleae, Rosaceae): Evidence from chloroplast genome and nuclear ribosomal DNA data using genome skimming. Mol. Phylogenet. Evol. 147, 106784 https://doi.org/10.1016/j.ympev.2020.106784.

Liu, B.-B., Ren, C., Kwak, M., Hodel, R.G.J., Xu, C., He, J., Zhou, W.-B., Huang, C.-H., Ma, H., Qian, G.-Z., Hong, D.-Y., Wen, J., 2022. Phylogenomic conflict analyses in the apple genus *Malus* s.l. reveal widespread hybridization and allopolyploidy driving diversification, with insights into the complex biogeographic history in the Northern Hemisphere. J. Integr. Plant Biol. 64, 1020–1043. https://doi.org/10.1111/jipb.13246.

Liu, H.-M., Schuettpelz, E., Schneider, H., 2020b. Evaluating the status of fern and lycophyte nothotaxa in the context of the Pteridophyte Phylogeny Group classification (PPG I). J. Syst. Evol. 58, 988–1002. https://doi.org/10.1111/jse.12641.

Liu, C., Shi, L.-C., Zhu, Y.-J., Chen, H.-M., Zhang, J.-H., Lin, X.H., Guan, X.-J., 2012. CpGAVAS, an integrated web server for the annotation, visualization, analysis, and GenBank submission of completely sequenced chloroplast genome sequences. BMC Genomics 13, 715. https://doi.org/10.1186/1471-2164-13-715.

Liu, S., Wang, Z., Wang, H., Su, Y., Wang, T., 2020. Patterns and rates of plastid *rps*12 gene evolution inferred in a phylogenetic context using plastomic data of ferns. Sci. Rep. 10, 9394. https://doi.org/10.1038/s41598-020-66219-y.

Liu, L., Yu, L., 2010. Phybase: An R package for species tree analysis. Bioinformatics 26, 962–963. https://doi.org/10.1093/bioinformatics/btq062.

Lohman, D.J., de Bruyn, M., Page, T., von Rintelen, K., Hall, R., Ng, P.K.L., Shih, H.T., Carvalho, G.R., von Rintelen, T., 2011. Biogeography of the Indo-Australian Archipelago. Ann. Rev. Ecol. Evol. Syst. 42, 205–226. https://doi.org/10.1146/annurev-ecolsys-102710-145001.

Lu, J.-M., Zhang, N., Du, X.-Y., Wen, J., Li, D.-Z., 2015. Chloroplast phylogenomics resolves key relationships in ferns. J. Syst. Evol. 53, 448–457. https://doi.org/10.1111/jse.12180.

Manchester, S.R., 2000. Late eocene fossil plants of the john day formation, wheeler county, oregon. Or. Geol. 62, 51–63.

Martín, M., Sabater, B., 2010. Plastid *ndh* genes in plant evolution. Plant Physiol. Biochem. 48, 636–645. https://doi.org/10.1016/j.plaphy.2010.04.009.

Matzke, N.J., 2014. Model selection in historical biogeography reveals that founder-event speciation is a crucial process in island clades. Syst. Biol. 63, 951–970. https://doi.org/10.1093/sysbio/syu056.

Matzke, N.J., 2018. BioGeoBEARS: BioGeography with bayesian (and likelihood) evolutionary analysis with R scripts. version 1.1.1. November 6, 2018 (GitHub, 2018).

Maurin, J.L.K., 2020. An empirical guide for producing a dated phylogeny with treePL in a maximum likelihood framework. arXiv:2008.07054v2.

McCoy, S., Kuehl, J., Boore, J., Raubeson, L., 2008. The complete plastid genome sequence of *Welwitschia mirabilis*: an unusually compact plastome with accelerated divergence rates. BMC Evol Biol. 8, 130. https://doi.org/10.1186/1471-2148-8-130.

Meleshko, O., Martin, M.D., Korneliussen, T.S., Schröck, C., Lamkowski, P., Schmutz, J., Healey, A., Piatkowski, B.T., Shaw, A.J., Weston, D.J., Flatberg, K.I., Szövényi, P., Hassel, K., Stenøien, H.K., 2021. Extensive genome-wide phylogenetic discordance is due to incomplete lineage sorting and not ongoing introgression in a rapidly radiated bryophyte genus. Mol. Biol. Evol. 38, 2750–2766. https://doi.org/10.1093/molbev/msab063.

Meng, H.-H., Song, Y.-G., 2023. Biogeographic patterns in Southeast Asia: Retrospectives and perspectives. Biodiv. Sci. 31, 23261. https://doi.org/10.17520/biods.2023261.

Miao, B.-B., Dong, W., Gu, Y.-X., Han, Z.-F., Luo, X., Ke, C.-H., You, W.-W., 2023. OmicsSuite: A customized and pipelined suite for analysis and visualization of multi-omics big data. Hortic. Res. 10, uhad195. https://doi.org/10.1093/hr/uhad195.

Min, Y., Guan, J., Li, S., Liu, S., Hong, Y., Wang, Z., Wang, T., Su, Y., 2018. The complete chloroplast genome of *Leptochilus hemionitideus*, a traditional Chinese medical fern. Mitochondrial DNA B Resour. 3, 784–785. https://doi.org/10.1080/23802359.2018.1491345.

Min, Y., Cai, S., Xiao, H., Zhang, M., Hong, Y., He, Z., Wang, Z., Wang, T., Su, Y., 2019. The complete chloroplast genome of *Pyrrosia calvata* (Polypodiaceae), a traditional Chinese medicinal fern only restricted to Guangxi. China. Mitochondrial DNA B Resour. 4, 1757–1758. https://doi.org/10.1080/23802359.2019.1610095.

Morales-Briones, D.F., Kadereit, G., Tefarikis, D.T., Moore, M.J., Smith, S.A., Brockington, S.F., Timoneda, A., Yim, W.C., Cushman, J.C., Yang, Y., 2021. Disentangling sources of gene tree discordance in phylogenomic data sets: Testing ancient hybridizations in Amaranthaceae s.l. Syst. Biol. 70, 219–235. https://doi.org/10.1093/sysbio/syaa066.

Moreau, C.S., Bell, C.D., Vila, R., Archibald, S.B., Pierce, N.E., 2006. Phylogeny of the ants: Diversification in the age of angiosperms. Science 312, 101–104. https://doi.org/10.1126/science.1124891.

Mower, J.P., Vickrey, T.L., 2018. Chapter nine—structural diversity among plastid genomes of land plants. In: Chaw S-M, Jansen RK, editors. Advances in botanical research. Vol. 85. Plastid genome evolution. London UK: Academic Press. pp. 263–292.

Myers, N., Mittermeier, R., da Mittermeier, C., Fonseca, G.A.B., Kent, J., 2000. Biodiversity hotspots for conservation priorities. Nature 403, 853–858. https://doi.org/10.1038/35002501.

Nelsen, M.P., Ree, R.H., Moreau, C.S., 2018. Ant-plant interactions evolved through increasing interdependence. Proc Natl Acad Sci U S a. 115, 12253–12258. https://doi.org/10.1073/pnas.1719794115.

Nguyen, L.T., Schmidt, H.A., von Haeseler, A., Minh, B.Q., 2015. IQ-TREE: A fast and effective stochastic algorithm for estimating maximum likelihood phylogenies. Mol. Biol. Evol. 32, 268–274. https://doi.org/10.1093/molbev/msu300.

Nie, Z.-L., Hodel, R., Ma, Z.-Y., Johnson, G., Ren, C., Meng, Y., Ickert-Bond, S.M., Liu, X.-Q., Zimmer, E., Wen, J., 2023. Climate-influenced boreotropical survival and rampant introgressions explain the thriving of New World grapes in the north temperate zone. J. Integr. Plant Biol. 65, 1183–1203. https://doi.org/10.1111/jipb.13466.

Nooteboom, H.P., 1997. The microsoroid ferns (Polypodiaceae). Blumea 42, 261–395.

Pease, J.B., Brown, J.W., Walker, J.F., Hinchliff, C.E., Smith, S.A., 2018. Quartet sampling distinguishes lack of support from conflicting support in the green plant tree of life. Am. J. Bot. 105, 385–403. https://doi.org/10.1002/ajb2.1016.

Pelosi, J.A., Kim, E.H., Barbazuk, W.B., Sessa, E.B., 2022. Phylotranscriptomics illuminates the placement of whole genome duplications and gene retention in ferns. Front. Plant Sci. 13, 882441 https://doi.org/10.3389/fpls.2022.882441.

Perrie, L.R., Field, A.R., Ohlsen, D.J., Brownsey, P.J., 2021. Expansion of the fern genus *Lecanopteris* to encompass some species previously included in *Microsorum* and *Colysis* (Polypodiaceae). Blumea 66, 242–248. https://doi.org/10.3767/blumea.2021.66.03.07.

Pillon, Y., 2012. Time and tempo of diversification in the flora of New Caledonia. Bot. J. Linn. Soc. 170, 288–298. https://doi.org/10.1111/j.1095-8339.2012.01274.x.

Potter, P.E., Szatmari, P., 2009. Global Miocene tectonics and the modern world. Earth-Sci. Rev. 96, 279–295. https://doi.org/10.1016/j.earscirev.2009.07.003.

Ppg, I., 2016. A community-derived classification for extant lycophytes and ferns. J. Syst. Evol. 54, 563–603. https://doi.org/10.1111/jse.12229.

Qi, X.-P., Kuo, L.-Y., Guo, C., Li, H., Li, Z.-Y., Qi, J., Wang, L.-B., Hu, Y., Xiang, J.-Y., Zhang, C.-F., Guo, J., Huang, C.-H., Ma, H., 2018. A well-resolved fern nuclear phylogeny reveals the evolution history of numerous transcription factor families. Mol. Phylogenet. Evol. 127, 961–977. https://doi.org/10.1016/j.ympev.2018.06.043.

Qian, Y., Meng, M., Zhou, C., Liu, H., Jiang, H., Xu, Y., Chen, W., Ding, Z., Liu, Y., Gong, X., Wang, C., Lei, Y., Wang, T., Wang, Y., Gan, X., Meyer, A., He, S., Yang, L., 2023. The role of introgression during the radiation of endemic fishes adapted to living at extreme altitudes in the Tibetan Plateau. Mol. Biol. Evol. 40, msad129. Doi: 10.1093/molbev/msad129.

Qu, X.-J., Moore, M.J., Li, D.-Z., Yi, T.-S., 2019. PGA: A software package for rapid, accurate, and flexible batch annotation of plastomes. Plant Methods 15, 50. https://doi.org/10.1186/s13007-019-0435-7.

Rambaut, A., 2017. FigTree-version 1.4.3, a graphical viewer of phylogenetic trees.

Ree, R.H., Smith, S.A., 2008. Maximum likelihood inference of geographic range evolution by dispersal, local extinction, and cladogenesis. Syst. Biol. 57, 4–14. https://doi.org/10.1080/10635150701883881.
Richardson, J.E., Bakar, A.M., Tosh, J., Armstrong, K., Smedmark, J., Anderberg, A.A., Slik, F., Wilkie, P., 2014. The influence of tectonics, sea-level changes and dispersal on migration and diversification of Isonandreae (Sapotaceae). Bot. J. Linn. Soc. 174, 130–140. https://doi.org/10.1111/boj.12108.
Ronquist, F., 1997. Dispersal-vicariance analysis: A new approach to the quantification of historical biogeography. Syst. Biol. 46, 195–203. https://doi.org/10.1093/sysbio/46.1.195.
Ronquist, F., Teslenko, M., van der Mark, P., Ayres, D.L., Darling, A., Höhna, S., Larget, B., Liu, L., Suchard, M.A., Huelsenbeck, J.P., 2012. MrBayes 3.2: Efficient Bayesian phylogenetic inference and model choice across a large model space. Syst. Biol. 61, 539–542. https://doi.org/10.1093/sysbio/sys029.
Salichos, L., Stamatakis, A., Rokas, A., 2014. Novel information theory-based measures for quantifying incongruence among phylogenetic trees. Mol. Biol. Evol. 31, 1261–1271. https://doi.org/10.1093/molbev/msu061.
Sayyari, E., Mirarab, S., 2016. Fast coalescent-based computation of local branch support from quartet frequencies. Mol. Biol. Evol. 33, 1654–1668. https://doi.org/10.1093/molbev/msw079.
Schneider, H., Kreier, H.P., Janssen, T., Otto, E., Muth, H., Heinrichs, J., 2010. Key innovations versus key opportunities: Identifying causes of rapid radiations in derived ferns. In: Glaubrecht, M. (Ed.), Evolution in Action. Springer, Berlin, pp. 61–75.
Schuettpelz, E., Pryer, K.M., 2009. Evidence for a Cenozoic radiation of ferns in an angiosperm-dominated canopy. Proc. Natl. Acad. Sci. u. s. a. 106, 11200–11205. https://doi.org/10.1073/pnas.0811136106.
Sears, B.B., 1980. Elimination of plastids during spermatogenesis and fertilization in the plant kingdom. Plasmid 44, 233–255. https://doi.org/10.1016/0147-619x(80)90063-3.
Shen, H., Jin, D., Shu, J.-P., Zhou, X.-L., Lei, M., Wei, R., Shang, H., Wei, H.-J., Zhang, R., Liu, L., Gu, Y.-F., Zhang, X.-C., Yan, Y.-H., 2018. Large scale phylogenomic analysis resolves a backbone phylogeny in ferns. GigaScience 7, 1–11. https://doi.org/10.1093/gigascience/gix116.
Smith, A.R., 1993. Phytogeographic principles and their use in understanding fern relationships. J. Biogeogr. 20, 255–264. https://doi.org/10.2307/2845633.
Smith, S.A., Moore, M.J., Brown, J.W., Yang, Y., 2015. Analysis of phylogenomic datasets reveals conflict, concordance, and gene duplications with examples from animals and plants. BMC Evol. Biol. 15, 1–15. https://doi.org/10.1186/s12862-015-0423-0.
Smith, S.A., O'Meara, B.C., 2012. treePL: Divergence time estimation using penalized likelihood for large phylogenies. Bioinformatics 28, 2689–2690. https://doi.org/10.1093/bioinformatics/bts492.
Smith, A.R., Pryer, K.M., Schuettpelz, E., Korall, P., Schneider, H., Wolf, P.G., 2006. A classification for extant ferns. Taxon 55, 705–731. https://doi.org/10.2307/25065646.
Song, Y.-Y., Cui, X.-S., Xu, L., Xing, Y.-P., Bian, C., Qiao, Y., Yang, Y.-Y., Kang, T.-G., 2021. The complete mitochondrial genome of *Dryopteris crassirhizoma* Nakai (Dryopteridaceae, Dryopteris Adanson). Mitochondrial DNA B Resour. 6, 2704–2705. https://doi.org/10.1080/23802359.2021.1966344.
Sukumaran, J., Holder, M.T., 2010. DendroPy: A python library for phylogenetic computing. Bioinformatics 26, 1569–1571. https://doi.org/10.1093/bioinformatics/btq228.
Sundue, M.A., Parris, B.S., Ranker, T.A., Smith, A.R., Fujimoto, E.L., Zamora-Crosby, D., Morden, C.W., Chiou, W.L., Chen, C.-W., Rouhan, G., Hirai, R.Y., 2014. Global phylogeny and biogeography of grammitid ferns (Polypodiaceae). Mol. Phylogenet. Evol. 81, 195–206. https://doi.org/10.1016/j.ympev.2014.08.017.
Suyama, M., Torrents, D., Bork, P., 2006. PAL2NAL: Robust conversion of protein sequence alignments into the corresponding codon alignments. Nucleic Acids Res. 34, W609–W612. https://doi.org/10.1093/nar/gkl315.
Swofford, D.L., 2002. PAUP*: Phylogenetic analysis using parsimony, version 4.0 b10. Sunderland, Massachusetts: Sinauer.
Testo, W.L., Field, A.R., Sessa, E.B., Sundue, M., 2019. Phylogenetic and morphological analyses support the resurrection of *Dendroconche* and the recognition of two new genera in polypodiaceae subfamily microsoroideae. Syst. Bot. 44, 1–16. https://doi.org/10.1600/036364419X15650157948607.
Testo, W., Sundue, M., 2016. A 4000-species dataset provides new insight into the evolution of ferns. Mol. Phylogenet. Evol. 105, 200–211. https://doi.org/10.1016/j.ympev.2016.09.003.
Than, C., Ruths, D., Nakhleh, L., 2008. PhyloNet: A software package for analyzing and reconstructing reticulate evolutionary relationships. BMC Bioinform. 9, 322. https://doi.org/10.1186/1471-2105-9-322.
Tillich, M., Lehwark, P., Pellizzer, T., Ulbricht-Jones, E.S., Fischer, A., Bock, R., Greiner, S., 2017. GeSeq – versatile and accurate annotation of organelle genomes. Nucleic Acids Res. 45, W6–W11. https://doi.org/10.1093/nar/gkx391.
Van Hinsbergen, D.J.J., Lippert, P.C., Dupont-Nivet, G., McQuarrie, N., Doubrovine, P.V., Spakman, W., Torsvik, T.H., 2012. Greater India Basin hypothesis and a two-stage Cenozoic collision between India and Asia. Proc. Natl. Acad. Sci. u. s. a. 109, 7659–7664. https://doi.org/10.1073/pnas.1117262109.
Van Uffelen, G.A., 1991. Fossil Polypodiaceae and their spores. Blumea 36, 253–272.
Van Uffelen, G.A., 1992. Sporogenesis in Polypodiaceae (Filicales). II. The genera *Microgramma* Presl and *Belvisia* Mirbel. Blumea 36, 515–540.
Van Uffelen, G.A., 1993. Sporogenesis in Polypodiaceae (Filicales). III. Species of several genera. Spore characters and their value in phylogenetic analysis. Blumea 37, 529–561.
Van Uffelen, G.A., 1997. The spore wall in Polypodiaceae: Development and evolution. In: Johns, R.J. (Ed.), Holttum: Memorial Volume. Royal Botanic Gardens Kew, London, pp. 95–117.
Vikulin, S.V., Bobrov, A.E., 1987. New fossil genus *Protodrynaria* (Polypodiaceae) from the Paleogene flora of Tim (the south of the Middle Russian upland). Botanicheskiy Zhurnal. 72, 95–98.
Vogel, J.C., Russel, S.J., Rumsey, F.J., Barrett, J.A., Gibby, M., 1998. Evidence for maternal transmission of chloroplast DNA in the genus *Asplenium* (Aspleniaceae, Pteridophyta). Botanica Acta. 111, 247–249. https://doi.org/10.1111/j.1438-8677.1998.tb00704.x.
Voris, H.K., 2000. Maps of Pleistocene sea levels in Southeast Asia: Shorelines, river systems and time durations. J. Biogeogr. 27, 1153–1167. https://doi.org/10.1046/j.1365-2699.2000.00489.x.
Walker, J.F., Brown, J.W., Smith, S.A., 2018. Analyzing contentious relationships and outlier genes in phylogenomics. Syst. Biol. 67, 916–924. https://doi.org/10.1093/sysbio/syy043.
Wang, K., Lenstra, J.A., Liu, L., Hu, Q.-J., Ma, T., Qiu, Q., Liu, J.-Q., 2018. Incomplete lineage sorting rather than hybridization explains the inconsistent phylogeny of the wisent. Comm. Biol. 1, 169. https://doi.org/10.1038/s42003-018-0176-6.
Wang, K., Duan, J., Ding, Y., Xiang, J.-Y., Liu, H.-M., 2021b. The complete chloroplast genome of *Platycerium wallichii* (Polypodiaceae), an endangered and ornamental fern species. Mitochondrial DNA B Resour. 6, 2313–2315. https://doi.org/10.1080/23802359.2021.1950057.
Wang, H.-X., Morales-Briones, D.F., Moore, M.J., Wen, J., Wang, H.-F., 2021a. A phylogenomic perspective on gene tree conflict and character evolution in Caprifoliaceae using target enrichment data, with Zabelioideae recognized as a new subfamily. J. Syst. Evol. 59, 897–914. https://doi.org/10.1111/jse.12745.
Wang, L., Qi, X.-P., Xiang, Q.-P., Heinrichs, J., Schneider, H., Zhang, X.-C., 2010a. Phylogeny of the paleotropical fern genus *Lepisorus* (Polypodiaceae, Polypodiopsida) inferred from four chloroplast DNA regions. Mol. Phylogenet. Evol. 54, 211–225. https://doi.org/10.1016/j.ympev.2009.08.032.
Wang, L., Wu, Z.-Q., Xiang, Q.-P., Heinrichs, J., Schneider, H., Zhang, X.-C., 2010b. A molecular phylogeny and a revised classification of tribe Lepisoreae (Polypodiaceae) based on an analysis of four plastid DNA regions. Bot. J. Linn. Soc. 162, 28–38. https://doi.org/10.1111/j.1095-8339.2009.01018.x.
Wang, Y.-R., Zhao, C.-F., Yu, X.-D., Zhang, X.-C., 2019. The complete chloroplast genome sequence of a typical alpine fern *Lepisorus waltonii* (Ching) S. L. Yu in Polypodiaceae. Mitochondrial DNA B Resour. 4, 801–803. https://doi.org/10.1080/23802359.2019.1574631.
Watkins Jr, J., Cardelús, C.L., 2012. Ferns in an angiosperm world: Cretaceous radiation into the epiphytic niche and diversification on the forest floor. Int. J. Plant Sci. 173, 695–710. https://doi.org/10.1086/665974.
Wei, X.-P., Wei, R., Zhao, C.F., Zhang, H.-R., Zhang, X.-C., 2017b. Phylogenetic position of the enigmatic fern genus *Weatherbya* (Polypodiaceae) revisited: Evidence from chloroplast and nuclear gene regions and morphological data. Int. J. Plant. Sci. 178, 450–464. https://doi.org/10.1086/692088.
Wei, R., Xiang, Q.-P., Schneider, H., Sundue, M.A., Kessler, M., Kamau, P.W., Hidayat, A., Zhang, X.-C., 2015. Eurasian origin, boreotropical migration and transoceanic dispersal in the pantropical fern genus *Diplazium* (Athyriaceae). J. Biogeogr. 42, 1809–1819. https://doi.org/10.1111/jbi.12551.
Wei, R., Yan, Y.-H., Harris, A.J., Kang, J.-S., Shen, H., Xiang, Q.-P., Zhang, X.-C., 2017. Plastid phylogenomics resolve deep relationships among Eupolypod II ferns with rapid radiation and rate heterogeneity. Genome. Biol. Evol. 9, 1646–1657. https://doi.org/10.1093/gbe/evx107.
Wei, R., Yang, J., He, L.-J., Liu, H.-M., Hu, J.-Y., Liang, S.-Q., Wei, X.-P., Zhao, C.-F., Zhang, X.-C., 2021. Plastid phylogenomics provides novel insights into the infrafamilial relationship of Polypodiaceae. Cladistics 37, 717–727. https://doi.org/10.1111/cla.12461.
Wei, R., Zhang, X.-C., 2022. A revised subfamilial classification of Polypodiaceae based on plastome, nuclear ribosomal, and morphological evidence. Taxon 71, 288–306. https://doi.org/10.1002/tax.12658.
Wickham, H., 2009. ggplot2: Elegant graphics for data analysis.
Wood, T.E., Takebayashi, N., Barker, M.S., Mayrose, I., Greenspoon, P.B., Rieseberg, L. H., 2009. The frequency of polyploid speciation in vascular plants. Proc. Natl. Acad. Sci. u. s. a. 106, 13875–13879. https://doi.org/10.1073/pnas.0811575106.
Woodruff, D.S., 2010. Biogeography and conservation in Southeast Asia: How 2.7 million years of repeated environmental fluctuations affect today's patterns and the future of the remaining refugial-phase biodiversity. Biodivers Conserv 19, 919–941. https://doi.org/10.1007/s10531-010-9783-3.
Wu, C., Lai, Y., Lin, C., Wang, Y., Chaw, S., 2009. Evolution of reduced and compact chloroplast genomes (cpDNAs) in gnetophytes: Selection toward a lower-cost strategy. Mol. Phylogenet. Evol. 52, 115–124. https://doi.org/10.1016/j.ympev.2008.12.026.
Yang, C.-H., Cui, Y.-X., Nie, L.-P., Wang, Y., Liu, X., 2020a. Chloroplast genomic analysis of *Pyrrosia assimilis*. Chin. J. Exp. Trad. Med. Formulae. 26, 123–131.
Yang, C.-H., Liu, X., Cui, Y.-X., Nie, L.-P., Lin, Y.-L., Wei, X.-P., Wang, Y., Yao, H., 2020b. Molecular structure and phylogenetic analyses of the complete chloroplast genomes of three original species of *Pyrrosiae* Folium. Chin. J. Nat. Med. 18, 573–581. https://doi.org/10.1016/S1875-5364(20)30069-8.
Yatabe, Y., Masuyama, S., Darnaedi, D., Murakami, N., 2001. Molecular systematics of the *Asplenium nidus* complex from Mt. Halimun National Park, Indonesia: Evidence for reproductive isolation among three sympatric *rbc*L sequence types. Am. J. Bot. 88, 1517–1522. https://doi.org/10.2307/3558459.
Yu, Y., Degnan, J.H., Nakhleh, L., 2012. The probability of a gene tree topology within a phylogenetic network with applications to hybridization detection. PLoS Genet. 8, e1002660.

Yu, Y., Blair, C., He, X.-J., 2020. RASP 4: Ancestral state reconstruction tool for multiple genes and characters. Mol. Biol. Evol. 37, 604–606. https://doi.org/10.1093/molbev/msz257.

Yu, Y., Nakhleh, L., 2015. A maximum pseudo-likelihood approach for phylogenetic networks. BMC Genomics 16, S10. https://doi.org/10.1186/1471-2164-16-S10-S10.

Zachos, J., Pagani, M., Sloan, L., Thomas, E., Billups, K., 2001. Trends, rhythms, and aberrations in global climate 65 Ma to present. Science 292, 686–693. https://doi.org/10.1126/science.1059412.

Zhang, D., Gao, F., Jakovlíc, I., Zou, H., Zhang, J., Li, W.-X., Wang, G.-T., 2020a. PhyloSuite: An integrated and scalable desktop platform for streamlined molecular sequence data management and evolutionary phylogenetics studies. Mol. Ecol. Resour. 20, 348–355. https://doi.org/10.1111/1755-0998.13096.

Zhang, L., Zhou, X.-M., Liang, Z.-L., Fan, X.-P., Lu, N.T., Song, M.-S., Knapp, R., Gao, X.-F., Sun, H., Zhang, L.-B., 2020b. Phylogeny and classification of the tribe Lepisoreae (Polypodiaceae; Pteridophyta) with the description of a new genus, *Ellipinema* gen. nov., segregated from *Lepisorus*. Mol. Phylogenet. Evol. 148, 106803 https://doi.org/10.1016/j.ympev.2020.106803.

Zhao, C.-F., Wei, R., Zhang, X.-C., Xiang, Q.-P., 2020. Backbone phylogeny of *Lepisorus* (Polypodiaceae) and a novel infrageneric classification based on the total evidence from plastid and morphological data. Cladistics 36, 235–258. https://doi.org/10.1111/cla.12403.

Zhong, B., Fong, R., Collins, L.J., McLenachan, P.A., Penny, D., 2014. Two new fern chloroplasts and decelerated evolution linked to the long generation time in tree ferns. Genome Biol. Evol. 6, 1166–1173. https://doi.org/10.1093/gbe/evu087.